Review

Catalyst Design and Engineering for Enhanced Microplastic Degradation and Upcycling - A Review

Chunxiang Zhu *, Ge Zeng, Pu-Xian Gao *

Posted Date: 12 September 2025

doi: 10.20944/preprints202509.1076.v1

Keywords: microplastic degradation; microplastic upcycling; catalyst design and engineering; photocatalysts

 doi:10.20944/preprints202509.1076.v1

Review

Catalyst Design and Engineering for Enhanced Microplastic Degradation and Upcycling - A Review

Chunxiang Zhu *, Ge Zeng and Pu-Xian Gao *

Department of Materials Science and Engineering & Institute of Materials Science, University of Connecticut

* Correspondence: puxian.gao@uconn.edu, chunxiang.zhu@uconn.edu

Abstract

Microplastics (MPs) are defined as "synthetic solid particles or polymeric matrices, with regular or irregular shape and with size ranging from 1 μm to 5 mm". They can originate from a variety of sources, such as synthetic textiles, city dust, tires, road markings, marine coatings, personal care products and engineered plastic pellets etc. During the lifetime of larger plastic debris, smaller and smaller pieces tend to form through degradation. Microplastics are challenging to collect and degrade due to its intrinsic chemical stability and small size. Despite being small in size, they are posing a great threat to both human beings and ecosystem. Besides, these tiny particles easily pass through water filtration systems and end up in the ocean and lakes, posing a potential threat to aquatic life. Extensive research has been conducted to find sustainable plastic alternatives or efficient removal approaches; while it remains in the early stage. To effectively mitigate the adverse effect caused by MPs, one of the solutions is through catalytic degradation with reduced time and energy demand and even gearing toward selective formation of useful products as a circular upcycling strategy. The catalytic approaches can be through photo, thermal, biological or electrochemical routes. Catalyst development for MPs degradation and upcycling lately has been actively conducted, however, a systematic and timely summary is lacking. Therefore, in this review, the design and engineering of novel catalysts with improved activity, selectivity, and stability especially for MPs degradation and upcycling are discussed, aiming to provide a thorough and timely reference for current status of MPs degradation catalysts, reaction mechanism, challenges and future opportunities.

Keywords: microplastic degradation; microplastic upcycling; catalyst design and engineering; photocatalysts

1. Introduction

Since the term MPs is firstly introduced in 2004 [1], its usage has been boosting due to increased awareness of MPs adverse effect to ecosystem and human being [2]. As shown in Figure 1a, number of papers published related to MPs has increased from 9 in 2011 to 3787 in 2024, showcasing a nearly 400 times increment. More and more attention has also been paid for efficient removal of MPs using catalysts (Figure 1b). MPs are an emergent yet critical issue for the environment because of their high degradation resistance and bioaccumulation [3,4]. Unfortunately, the current technologies to remove, recycle, or degrade MPs are insufficient for their complete elimination [5,6]. In addition, the fragmentation and degradation of mismanaged plastic wastes in environment have been also identified as a significant source of MPs [7], making sustainable MPs managing an urgent need. Thus, the developments of effective MPs removal methods, as well as, plastics recycling strategies are crucial to build a MPs-free environment.

 doi:10.20944/preprints202509.1076.v1

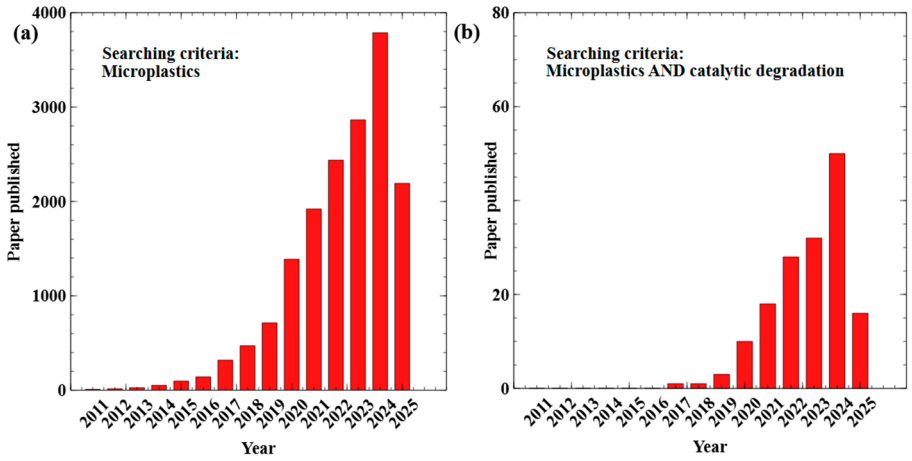

Figure 1. Number of papers published each year in the past 15 years related to (a) Microplastics in general and (b) Catalytic degradation of microplastics. Source: Web of Science. Data collected on 08-19-2025. Searching criteria is listed in the plot.

MPs refer to the plastics with size ≤5 mm and can be further divided into more defined categories, including micro-size, nano-size, and even pico-size [8]. Until now, there is still no consensus for the upper and lower limit of the MPs size [9]. Based on the origin, MPs could be generated from two approaches. One is primary MPs which are used in cosmetics, paint or pellets and flakes for plastic products generation. Primary MPs are intentionally manufactured and added to products. Common examples include microbeads in cosmetics, plastic pellets used in manufacturing, and microfibers in textiles etc. The other way is secondary MPs which are produced from larger plastic products during use and under weathering, such as wearing of textiles and tires, fragmentation of larger piece under UV and biological interaction [3,10]. MPs can be redistributed by wind, rain, and water and finally end up in large water body (lake and ocean), as shown in the life cycle of MPs in Figure 2. The small size of MPs makes them easily entering living organism from top to bottom of food chain. While their pervasive nature further increases the bioaccumulation [11]. Toxicity of MPs has been widely observed and identified across terrestrial and aquatic ecosystems. Behavioral, metabolic, and developmental changes could happen with MPs exposure [12]. Adverse effects including survival rate of Zooplankton, altered finfish behavior [13], clam eggs hatching [14], and urchin physical abnormalities [15] have been reported. With prolonged consumptions of MPs, digestive tracts blocking, digestive behavior disorder, and even reproductive capability impairment could happen for whole organisms in the food chain [16].

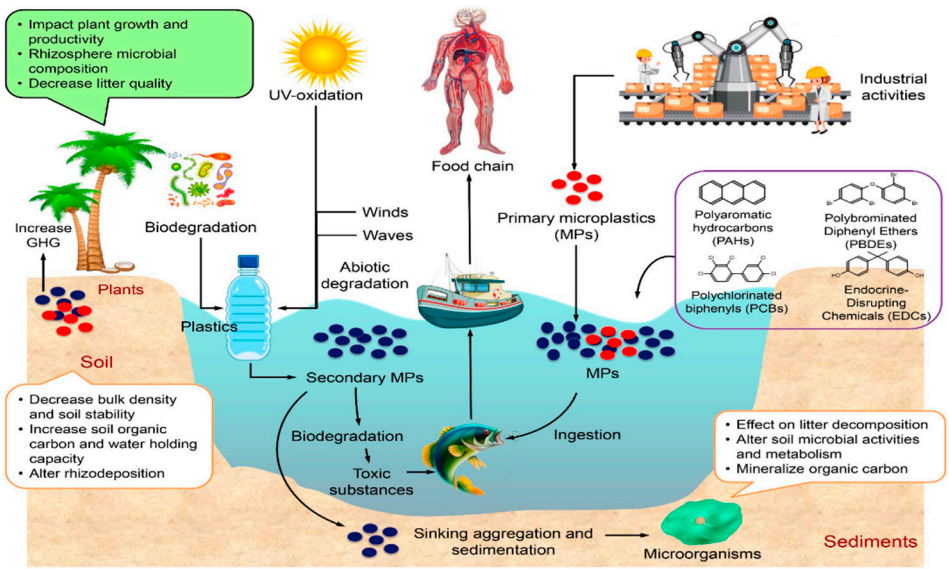

 doi:10.20944/preprints202509.1076.v1

Figure 2. A life cycle demonstration of MPs, including formation of primary and secondary MPs, adverse effects of their formation on aquatic flora and to human through the food chain [16].

Therefore, identifying effective strategies to mitigate the accumulation of environmental MPs is crucial, given its direct implications for both human health and ecosystem sustainability. In this regard, catalytic MPs handling shows great promise. Recent studies have highlighted several advantages of catalytic MP degradation over conventional treatment methods (filtration, coagulation-flocculation, and sedimentation etc.). According to literature [17], the estimated half-lives for HDPE can range from 58 years (bottles) to 1200 years (pipes) in the natural marine environment. In the regards, catalytic processes demonstrate high efficiency in accelerating polymer breakdown under relatively mild and environmentally compatible conditions, including ambient temperature [18], atmospheric pressure [19], and visible light irradiation [20]. In addition, catalysts offer improved selectivity and control, allowing for targeted degradation pathways while minimizing the formation of undesirable by-products [21]. A further benefit lies in the potential conversion of MPs into value-added products, such as fuels or chemical feedstocks [22], coupling environmental remediation with resource recovery. Moreover, catalytic approaches reduce the likelihood of generating secondary pollutants and show strong potential for scalability through advances in nanocatalyst design and reactor engineering. Collectively, these advantages underscore the promise of catalytic degradation as a sustainable strategy for mitigating MPs pollution.

As the title suggests, this work centers on catalyst development and engineering specifically aimed at MPs degradation. While extensive research has been devoted to catalyst design for bulk plastic recycling and upcycling, studies on catalytic processes for MPs remain relatively limited due to the unique physicochemical properties of MPs and the challenges associated with their collection. Accordingly, this review focuses exclusively on studies involving catalytic degradation of MPs, whereas research on macro-scale plastic catalytic degradation is either excluded or used only as a comparative reference. To establish a foundation for catalyst development in this field, the review first outlines the key differences between MPs and bulk plastics. It then briefly discusses methods for MPs identification and quantification, given that accurate evaluation of catalyst performance depends closely on these techniques. Section 4 provides a detailed overview of current catalytic degradation approaches for MPs—including photochemical, biological, electrochemical, thermochemical, and hybrid chemical pathways—with particular emphasis on catalyst-assisted processes that enhance degradation rates and performance. Building on this, the underlying mechanisms are examined to highlight the fundamental principles of catalyst design and engineering. Finally, the review lists current challenges and explores future opportunities in catalytic MPs degradation, with the aim of offering insights and inspiration for subsequent research in this emerging area.

2. Difference Between MPs and Bulk Plastics

Before getting into the catalyst's development for efficient MPs degradation, it is important to understand the differences between bulk plastics and MPs. Degradation, recycling, and upcycling of bulk plastics have been extensive studied through pyrolysis, gasification, reprocessing and photo-reforming [23–25]. Theoretically, the catalysts that have been developed and tested for bulk plastics' treatment could be extended to MPs. While, there are still many questions remaining to be answered as many differences existing between bulk material and their size reduced counterparts. As the name implies, the major difference between bulk plastics and MPs is the size. Size of MPs can span a wide range, from nm to mm (as shown in Table 1), making them hard to detect, observe, collect, and study, especially with current commercially available methods. Due to the small size of MPs, they can be easily taken in by living organisms and widely distributed from organic to inorganic substances, from soil to water, from deep in the sea to top of mountain [26]. Therefore, mixed methodologies need to be applied for catalyst performance evaluation based on MPs with different conditions.

 doi:10.20944/preprints202509.1076.v1

Table 1. MPs size class nomenclature with their respective size range, and organisms of equivalent size in the environment. Modified from work [27].

Current size categories	Size range	Proposed size categories	Size Range	Organism of equivalent size
Nanoplastic	0.001–1 μm	Femto-size plastics	0.02–0.2 μm	Virus
Microplastic	1–1000 μm	Pico-size plastics	0.2–2 μm	Bacteria
		Nano-size plastics	2–20 μm	Flagellates
		Micro-size plastics	20–200 μm	Diatoms
Mesoplastic	1–10 mm	Meso-size plastics	200–2000 μm	Amphipods
Macroplastic	> 1 cm	Macro-size plastics	0.2–20 cm	Jellyfish
		Mega-size plastics	20–200 cm	Jellyfish

Besides the size, the second difference of MPs is their complexity both in physical and chemical properties. MPs can originate from numerous sources and are usually treated as heterogeneous materials, including synthetic clothing, microbeads, and breakdown of larger plastic items. Their variation in size, shape, density, and chemical composition, makes their studies complicated not only in detection, but also in removal methodologies development. In the work of MPs identification from beaches Plymouth UK by Richard Thompson et al. [1], 9 polymers are identified including acrylic, alkyd, polyethylene, polypropylene, polyamide, polyester, polyethylene, polymethylacrylate, polypropylene, and polyvinyl-alcohol, indicating that the MPs come from different bulk plastic sources. Besides, for the origin of MPs toxicity, it can be a result of the plastic chemicals or the particle itself. While, different MPs can show significantly difference in toxicity. According to the work from Lisa Zimmermann et al. [28], the authors show that chemicals in plastics contribute more for toxicity in the case of the PVC but not of the PUR and PLA plastics. Interestingly, they observed that bioplastics show similar toxicity as its conventional plastics counterpart. Therefore, treating MPs as a homogenous entity is not suitable for environmental impact assessment. Instead, the chemical compositions and physical conditions of different MPs should be considered. Thereof, it will be much more challenging to develop efficient catalysts for the heterogeneous MPs treatment compared to their bulk counterparts. For a better view, properties change of macro plastics to MPs after degradation are summarized and shown in Figure 3. A detailed properties comparison between bulk plastic and MPs is provided in Table 2.

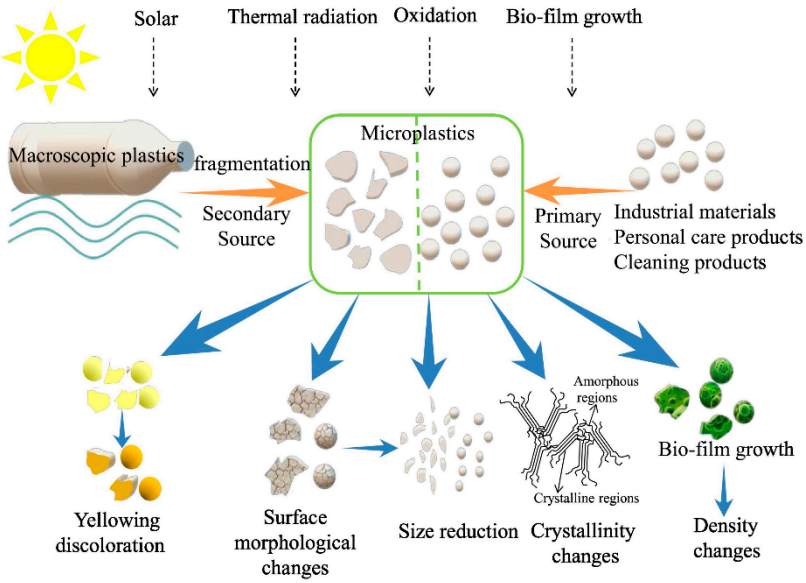

Figure 3. Properties changes of microplastics after degradation [29].

 doi:10.20944/preprints202509.1076.v1

Moreover, MPs present varied chemical properties due to their high energy surface through degradation processes. With a large surface area-to-volume ratio, MPs can readily adsorb pollutants from the surrounding environment through hydrophobic interactions sorption mechanism, through electrostatic forces, van der Waals forces, hydrogen bonding, and pi-pi interactions [30]. These adsorbed chemicals can include persistent organic pollutants (POPs), heavy metals, and other toxins, not only increasing the harmful potential of the ingested plastics to the ecosystem, but also for their catalytic recycling. The aging process of plastics, leading to MPs formation, can also modify their surface properties and crystallinity, affecting their ability to adsorb and desorb pollutants. Since MPs are usually generated from bulk plastic degradation, physical and chemical properties, such as color, surface morphological, crystallinity, particles size, and density of MPs are usually different compared to the bulk materials [29].

Table 2. Properties comparison between bulk plastic and microplastic.

Category	Bulk plastic	Microplastic
Origin	Intentionally manufactured	MPs are either produced at that size (primary microplastics) or result from the fragmentation of larger plastic waste (secondary microplastics) through aging, weathering and fragmentation
Size	> 5 mm	< 5 mm, no lower limit yet
Shape	Varied shapes can be controlled	Fragments, fibers, films, foams, and microbeads. The shapes can be broadly categorized as regular (spherical, cylindrical, etc.) or irregular
Polymer type	Single type or with controlled polymer types	MPs can be composed of a wide variety of polymer types as a mixture. The most common include polyethylene (PE), polypropylene (PP), polystyrene (PS), polyethylene terephthalate (PET), and polyvinyl chloride (PVC). Other polymers like polyamide (PA), polyurethane (PU), polycarbonate (PC), and polyester (PES) are also found in microplastics. The specific polymers found in microplastics can vary depending on the source and location.
Surface	Low surface to volume ratio	Higher surface area to volume ratio, higher surface energy. Higher surface charge due to ions absrobtion. May include cracks, pits, and other surface features due to UV radiation, mechanical abrasion, and chemical degradation.
Crystallinity	Standard and uniform	Weathering and aging processes can significantly alter the crystallinity of microplastics
Surface chemistry	Relative clean	Absorbed substances from the environment, including pollutants (organic, inorganic), nutrients, and microorganisms, leading to changes in their surface properties and behavior. Presence of specific functional groups on the surface (e.g., hydroxyl, carboxyl)

3. Microplastic Identification and Quantification

Precise identification and quantification of MPs before and after in the catalytic process is vital for the catalyst's performance evaluation. However, this is not an easy task due to the complicated chemical and physical properties of MPs and interference from other similar micro substances. In this section, techniques that can be used for MPs identification and quantification are summarized and discussed.

 doi:10.20944/preprints202509.1076.v1

The selection of MPs identification and quantification methods depends largely on particle size and matrix complexity. For particles >100 μm, optical microscopy enables rapid visualization of morphology, size distribution, and color, though often requiring sediment and physical sieving [31,32]. For <100 μm particles, resolution limits of optical microscopy reduce reliability, and electron microscopy (SEM) provides detailed structural insights with the help of EDS, it is worth mentioning that unlike the traditional processing methods for non-conductive samples, wet-mode imaging avoided the introduction of other elements during the coating process, thereby enhancing the identification capability of SEM/EDS for microplastics [33].

Among chemical methods, FTIR remains the most widely applied, with focal plane array (FPA)-based imaging enabling large-scale mapping. It is effective for >20 μm particles but less sensitive to nanoplastics and prone to spectral fouling [34,35]. Raman spectroscopy is effective for <20 μm particles and is less affected by water interference, though fluorescence back-ground remains a challenge [36]. ^{1}H NMR provides quantitative compositional and degradation information of microplastic particle that <300 μm but requires large sample quantities, restricting routine use [37–39].

Thermal and mass-based approaches, including Py-GC/MS and TGA, are powerful for compositional analysis. Unlike the above methods, they are not limited by the particle size. By identifying certain additives or molecular markers, they can indicate the origin of specific plastics, providing evidence for analyzing samples with complex microplastic components [40]. Py-GC/MS identifies polymers via characteristic pyrolytic fragments, while TGA provides thermal degradation profiles. Both require dried, homogenized samples and offer robust quantitative data, although they are destructive and can-not preserve morphology [41].

Pretreatment strategies vary across methods: microscopy relies mainly on physical separation such as sedimenting [31,33]; FTIR and Raman require density separation and dry on the anodisc filters [35], NMR demands bulk concentration [38]; and thermal/mass-based methods depend on drying and homogenization which are usually more than complex depend on specific situation [42]. In terms of MPs identification and quantification, no single technique yet is sufficient for a comprehensive characterization. Table 3 lists a simple comparison between different techniques used for MP identification and quantification. Figure 4 presents current and novel technologies that can be used for MPs detection in different environment.

Table 3. Comparison summary between different techniques used for MP identification and quantification.

Method	Advantages	Limitations	Particle Size Best Suited For	Typical Pretreatment Steps
Optical Microscopy	Rapid visualization; low cost; simple operation	Limited resolution; cannot identify polymer type	>100 μm	Filtration/sieving; density separation
SEM/EDS	Very high resolution; reveals surface structure and aggregation	Cannot identify polymer type; expensive instrumentation;	<100 μm	Filtration/digestion → drying → conductive coating (Au/C) or wet-mode imaging
μ-FTIR / FPA-FTIR	Enables polymer identification; FPA allows batch imaging/statistics; high throughput	Low sensitivity for nano plastics; easily disturbed by environmental fouling	>20 μm	Filtration onto IR-transparent substrates; H_2O_2 or enzymatic digestion
Micro-Raman	High spatial resolution (sub-micron detection); less affected by water	Strong fluorescence background; long acquisition time; high instrument cost	<20 μm	Clean low-fluorescence filters; filtration
^{1}H NMR	Rich quantitative information: polymer composition, degradation pathways, additives	Requires large sample amounts; expensive; not suitable for routine monitoring	<300 μm	Bulk sample concentration; solvent extraction
Py-GC/MS (incl. TED-GC/MS)	Accurate qualitative/quantitative identification of polymers in	Destructive method; no morphological information	No limitation on particle size	Drying; homogenization; removal of salts/water

 doi:10.20944/preprints202509.1076.v1

	mixed or weathered samples; improved throughput			
TGA	Characterizes thermal degradation behavior; combined with FTIR/MS gives composition and quantification	Overlapping thermal peaks; interference from organics or minerals	No limitation on particle size	Drying; homogenization; removal of inorganic/organic matter

Often times, all the aforementioned methods need to be paired and cross-verified to achieve a robust evaluation for MPs study. In the work of Thava Palanisami et al. [43], a combined technique using SEM, BET, XRD, ATR-FTIR, and TGA is applied to study the long-term degradation of MPs in the marine environment in terms of their surface morphology, surface area, surface chemical species, crystallinity, and stability changes. In another work of measuring fragmentation rates of MPs [44], the authors include the analytical ultracentrifugation with a refractive index detector (AUC-RI), a single-particle counter, for particle size distribution, and concentration quantification. The particle shape is characterized using SEM. While ultraviolet–visible spectroscopy (UV–vis) is applied for monitoring the content of released water-soluble organics (total organic carbon, TOC).

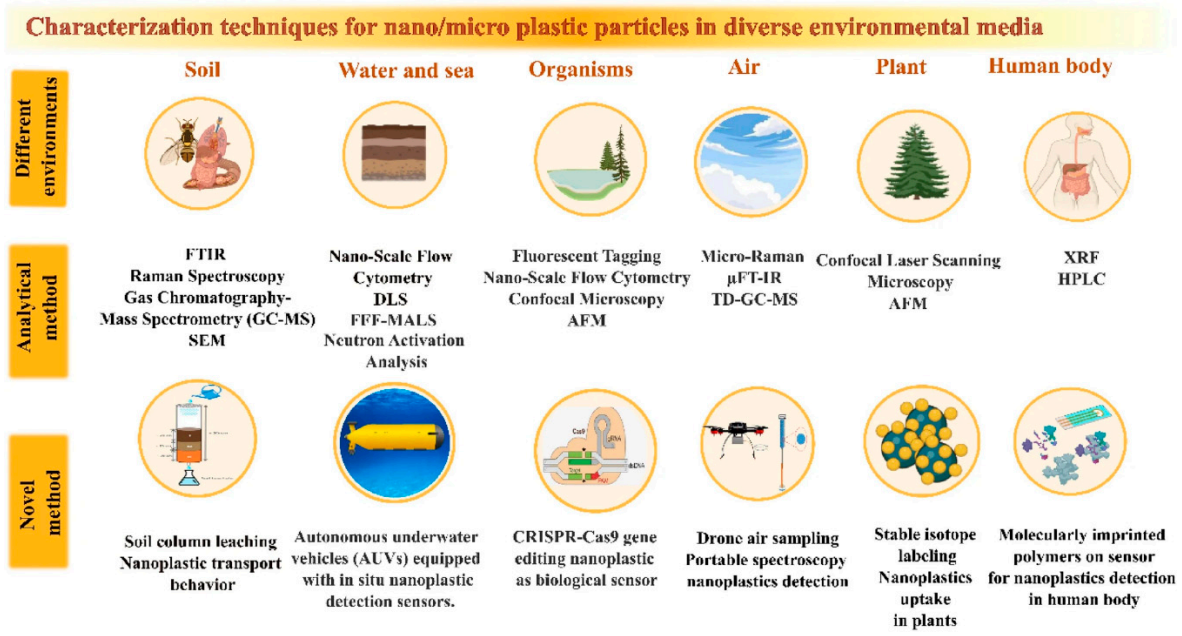

Figure 4. Summary of current and novel technologies that can be used for MPs detection in different environment [45].

4. Enhanced Microplastic Degradation Using a Catalyst

MPs degradation includes transforming MPs into smaller molecules that are less harmful or useful components, such as CO_2 [46], light hydrocarbons [47], carbon-based materials for catalyst preparation [48], fuel, and chemicals [49], etc. Under natural environmental conditions, the MPs degradation process is slow and results in a loss of carbon stock due to their persistent nature and a lack of reaction control. To mitigate the challenges and potentially turn wasted MPs into valuable feedstock back into the carbon cycle, catalysts play a vital role to speed up the degradation process and control the reaction direction. In the review, depending on the working mechanism and materials type used, catalysts for MPs degradation are divided into photocatalysts, Fenton and Fenton-like catalysts, thermochemical catalysts, bio and bio-inspired catalysts, electrocatalysts, and hybrid catalysts, aiming to provide a clear and systematic overview for currently applied MPs catalysts. Based on the category, novel catalyst design and engineering methods used to achieve improved MPs degradation will be summarized and discussed based on the most recent publications.

 doi:10.20944/preprints202509.1076.v1

4.1. Photocatalysts

Current mostly often used photocatalysts for MPs degradation include TiO_2 [50], ZnO [51], graphite carbon nitride (g-C_3N_4) [52], and metal organic framework (MOF) etc. These materials work by generating reactive oxygen species (ROS) when activated by light, which then break down the polymer chains of MPs into smaller, less harmful components, ultimately aiming for mineralization into CO_2 and H_2O. Besides the conventional materials, bismuth-based catalyst [53], Mxene based materials, and plasmonic metal nanoparticles like Au and Ag can enhance light absorption and catalytic activity, resulting in superior performance. A more detailed summary of photocatalysts used for MPs degradation can be found in the review paper [54].

Mechanism: Usually, three steps are involved in a general photocatalytic process: (1) charge carriers' generation from semiconductor photocatalyst through photon energy activation; (2) charge carriers transfer from bulk to surface of photocatalysts and (3) photogenerated charge carriers induce surface redox reaction on the target [55]. In photocatalysis, semiconductors are usually used and act as photocatalysts by absorbing photon energy, becoming excited, and generating electron-hole pairs and ROS. These ROS, including hydroxyl radicals (·OH) and superoxide ions (O_2·−), play a crucial role in the degradation of MPs [56]. In terms of MPs photocatalytic degradation mechanism, the process includes mainly four steps: (1) chain initiation, (2) chain growth, (3) chain branching, and (4) chain termination. For the initiation of MPs degradation, two pathways have been proposed. In the first route, the strong oxidative holes (h^+) in the catalyst VB can oxidize MPs, leading to CO_2 and H_2O generation. Alternatively, the excited e^- and h^+ can react with O_2 and H_2O on the surface of the photocatalyst, generating primarily ·OH and O_2·−.

The photocatalytic MPs treatment can be divided into three categories: photo-degradation, photo-conversion, and photo-reforming [57] as shown in Figure 5. For photo-degradation, CO_2 as a mineralization product is produced through a non-selective oxidation processes which occurs in an aerobic environment. While, value added chemicals and fuels are generated through photo-reforming and photo-conversion processes which are typically in an anoxic condition. At the same time, side products such as H_2, formate, acetate acid, and other valuable chemicals [58–60] can also be produced through photo-reforming and photo-conversion using the remaining electrons in the system.

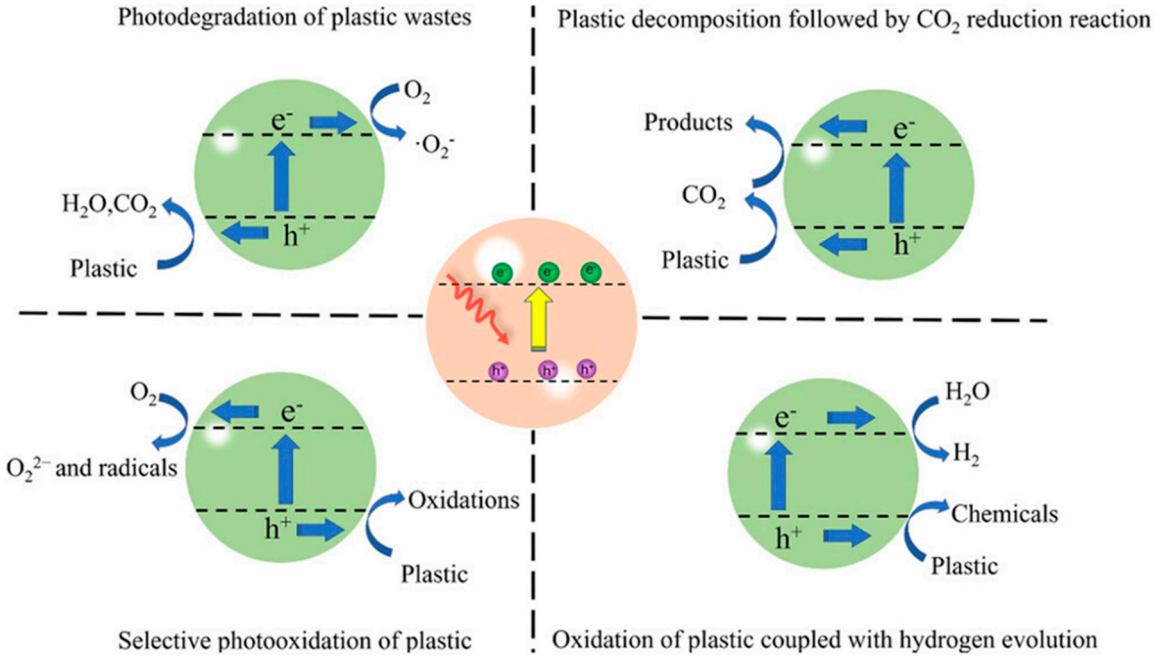

Figure 5. Mechanism summary of photocatalytic plastic conversion pathways including photo-conversion, photo-degradation, and photo-reforming with different products generation [57].

 doi:10.20944/preprints202509.1076.v1

To improve photocatalytic performance, one of the effective ways is to construct heterostructures with other semiconductors, activated carbon, graphene or noble metals. Slamet et al. [61] prepared an Ag/TiO_2 nano-composites. The catalyst is used for simulated MP particles degradation in water under UV light. 50 mg of the catalyst is added for 100 ppm of PE MP decomposition. The results show that 100% MP degradation within 120 min can be achieved. While MP with particle size between 125-150 micrometers shows the fast degradation rate with 100% degradation efficiency in 90 min irradiation. Similarly, g-C_3N_4/TiO_2/WCT-AC composite was prepared using waste cotton based activated carbon (WCT-AC) loaded TiO_2 as precursor [58]. Through the heterojunctions construction, improved visible light absorption and photoelectron-hole separation can be achieved, resulting in a 67.58% of PE degradation in 200h under visible light conditions. Same engineering approach has also been applied by synthesizing a Pt-ZnO nanocomposite [62] for LDPE film photodegradation. The photocatalysis testing of LDPE film (1 cm × 1 cm) is conducted in DI water under visible light for 175 h. Through FTIR characterizations, the authors indirect quantify the degradation content using carbonyl and vinyl indices (CI and VI). In average, there is a 13% and 15% increase respectively for CI and VI, indicating an increased degradation performance using Pt-ZnO combination. Besides, LDPE showcased deeper cavities and wrinkles formation after 175 h visible light irradiation compared to the original smooth surface. Heterojunctions of MXene based photocatalyst composite has also been developed for H_2 evolution integrated with enhanced PET degradation [60]. By successfully constructing MXene/$Zn_xCd_{1-x}S$ photocatalysts through a band structures engineering approach, simultaneously H_2 production with a rate of 14.17 mmol·g^{-1}·h^{-1} and PET degradation can be achieved. What is more, organic valuable micro-molecule compounds, such as glycolate, acetate and methanol, etc. can also be produced, demonstrating a superb photocatalyst development scheme. WO_3/g-C_3N_4 as a composite photocatalyst has also been synthesized via a hydrothermal method to do the same work [59]. With a 30% WO_3/g-C_3N_4 formula, a high H_2 evolution rate of 14.21 mM and PET degradation to formate, methanol, acetic acid, and ethanol can be realized under visible light. Creating a heterojunction between WO_3 and g-C_3N_4, improved photocatalytic performance can be achieved due to the reduced recombination of charge carriers and the enhanced redox capability. Catalyst structure can be another factor to tune. Core-shell BiO_{2-x}/$CuBi_2O_4$ heterojunction is constructed [63]. Increased PE and PS MPs degradation can be achieved, due to an elevated electron transfer from $CuBi_2O_4$ to BiO_2 with a built-in electric field, facilitating efficient electron flow.

Besides heterojunctions construction, doping offers another promising strategy to alter the photoelectron-hole pair recombination. To mitigate the issue facing Bismuth based photocatalysts, a novel Fe-doped BiO_{2-x}/BiOI heterojunction photocatalyst was developed through a chemical precipitation method [53]. Due to a Z-scheme heterojunction construction and impurity Fe introduction, increased redox abilities and electron-hole pairs separation can be achieved, resulting in elevated PET degradation within 10 h under full-spectrum light. In another work, Nb-doped SnO_2 quantum dots (QDs) were prepared by a hydrothermal process [64], aiming to generate a synergistic effect using dual defects engineering. Nb impurities and the introduced oxygen vacancy extend the conduction band edge to the Fermi level, narrowing the bandgap and providing abundant defect states for electron transitions. Finally, a 28.9% PE MPs weight loss can be achieved after 7 h photo irradiation. Using doped photocatalysts, elevated MPs degradation can be acquired by coupling photo and electrical methods. TiO_2-modified boron-doped diamond photoanode has been prepared for the purpose [65]. HDPE MPs degradation was performed using electrochemical oxidation and photoelectrocatalysis (PEC) on bare and modified BDD electrodes both under dark and UV light conditions. The results show that 89.91 ± 0.08% of HDPE MPs degradation in 10-h can be achieved and is more efficient at a low current density (6.89 mA/cm).

Morphological modification and surface sensitization represent another effective design approach of promoting photocatalytic MPs degradation efficiency. Spherical and nanosheet Bismuth oxychloride (BiOCl) have been prepared, aiming to study the catalyst morphology effect on MPs degradation [66]. The results showed that BOC-N nanosheets achieved a 44.33% degradation of PET

 doi:10.20944/preprints202509.1076.v1

MPs within 5h, ascribing to the easy transfer of photogenerated carriers to the surface. Titania coated 3D ZnO tetrapods were also prepared for photocatalytic degradation of PE and polyester (PES) MPs [67]. Complete PE and PES degradation is achieved under UV illumination for 480 h and 624 h respectively. The authors found that the MPs morphology can affect the degradation rate and use of electron scavengers is necessary. MPs surface modification can also play an important role. In the work of Jiang et al. [68], PS MPs were modified by different functional groups, including –OH, $–NH_2$, $-SO_3H$, –COOH and -epoxy. Photocatalytic degradation was conducted using a BiOBr-OH semiconductor-organic framework. The results showed that surface modification increased the polarity of MPs surface, resulting a sluggish degradation rate. Therefore, the PS-plain MPs without any treatment showed the highest degradation rate. Via phase transformation and sulfur vacancy engineering, Edalati and colleagues introduce a highly efficient cadmium sulfide (CdS) photocatalysts which dramatically improve H_2 production and PET MPs degradation [69]. Using hydrothermal treatment and high-pressure processing, parent CdS can be converted into a thermodynamically stable wurtzite (hexagonal) phase with abundant sulfur vacancies generation at the same time. These sulfur vacancies serve as active catalytic sites that facilitate enhanced photocatalytic performance. 23-time increase in both H_2 production and PET degradation can be achieved compared to the commercial CdS.

A table summary of catalyst materials, reaction condition and performance for photocatalytic MP degradation is shown in Table 4. It can be learnt that semiconductors and their modified counterparts are mostly used photocatalysts for MPs degradation. Current photocatalytic MPs degradation focuses on lab scale demonstration with single and controlled MPs environment. Besides, in most of the work, MP degradation efficiency is calculated by using a weight change measurement. However, based on the low MP concentration used. It is questionable how accurate the quantification method can be, raising a concern for the final performance demonstration. Last but not least, the use of a lab-controlled environment in the photocatalytic testing is suitable for scientific investigation but lacks relevance to real-world applications. This is extremely important considering a practical solution to tackle the existing MPs adverse effect is in urgent need. For more information about current status, challenges and future direction for MPs photocatalytic degradation, the following reviews [70–72] can be referred.

Table 4. Summary of catalyst, reaction condition and performance for photocatalytic MP degradation.

Catalyst	MP type	Size	Condition	Products	Quantification method	Efficiency	Ref.
Fe-doped BiO_{2-x}/BiOI heterojunction	PET	NA	Xenon lamp (200–1000 nm, 500W) in water	NA	Degradation efficiency by FT-IR characterization	NA	[53]
g-C_3N_4/TiO_2/WCT-AC	PE	0.15 mm	500W xenon lamp irradiation for 200 h in water at 25 °C with 600 rpm	NA	Weight loss	67.58 % revmoal in 200h	[58]
C_3N_4/WO_3	PET	0.45 μm	300W xenon lamp at 25 °C in water	H_2: 14.21 mM and formate, methanol, acetic acid, and ethanol	Weight loss was measured	NA	[59]
MXene/$Zn_xCd_{1-x}S$	PET solution	NA	300W Xenon lamp, reaction in 50 ml PET solution	14.17 mmol·g^{-1}·h^{-1} H_2 generation rate. Glycolate, acetate, ethanol, etc.	HNMR spectroscopy	NA	[60]
Ag/TiO_2 nano-composites	PE	100-250 μm	UV lamp irradiation with 2000 rpm	NA	Weight loss was measured	100% in 90 min for 125-200 μm	[61]
Pt/ZnO nanorods	LDPE	50 μm	50W dichroic halogen lamp, 175h	NA	Carbonyl index (CI) and vinyl index (VI) calculation through FTIR	13% and 15% increase for CI and VI with Pt compared to ZnO only	[62]
Core-shell BiO_{2-x}/$CuBi_2O_4$ heterojunction	PS and PE	4 μm	Full spectrum light sources (300W, Xenon lamp	Benzoic acid, ethylbenzene and styrene	FTIR was used to quantify the carbonyl content	Severe damage to the surface PS after 15d of full spectrum light irradiation compared to BiO_{2-x} and $CuBi_2O_4$ alone	[63]
Nb doped SnO_2 quantum dot	PE	350 μm	Visible light from an 8W LED (400–800 nm) and a 200W Xe lamp (380–1100 nm)	CO_2 and H_2O with HC intermediates	Weight loss	28.9% weight loss after 7 h	[64]
TiO_2-modified boron-doped diamond (BDD/TiO_2)	HDPE	250 μm	6.89 mA cm^{-2} current density and UV light in aqueous media	Organic compounds such as aldehydes and ketones	FTIR was used to quantify the carbonyl content	89.91±0.08% of HDPE MPs in a 10-h	[65]
BOC-S, BOC-N and BiOCl photocatalysts	PET	37 μm	180 °C for 12 h. 300W xenon lamp	CO_2	Weight loss	44.33% degradation of PET MPs within 5 h.	[66]
TiO_x/ZnO tetrapod	PE and PES microfibers	100 μm	365 nm UV light at room temperature	NA	Weight loss	Complete mass loss of PE and PES under UV illumination for 480 h and 624 h	[67]
BiOBr-OH semiconductor-organic framework	PS	5 μm	250W Xe lamp for 72 h	Monomeric molecules and multiple molecular complexes	Weight loss, filter with 1 μm filter paper	7.31% mass loss after 72 h	[68]
S vacancy-rich CdS	PET	~500 μm	Simulated solar irradiation 6h	H_2, Terephthalic acid, Ethylene glycol, Formic acid	Mass Loss and GC	23-fold increase in H_2 production compared to commercial CdS	[69]
BiOI-MOF composite	PE	230±90 μm	500W Xenon lamp for 6 h	Alcohols, lipids, carboxylic acids, long-chain alkane	ATR-FTIR for cabornyl	CI decreased to 0.127 in 6 h	[73]
TiO_2 anchored chitin sponge	PS	1 μm	60W lamp (λ = 365 nm), UV light	2-Butanone, 3,3-dimethyl cyclohexanone	UV-vis dye assissted quantification	58.4% in 6h	[74]

 doi:10.20944/preprints202509.1076.v1

4.2. Fenton and Fenton-like Catalysts

Beyond photocatalysis, Fenton and Fenton-like reactions represent the second most widely applied approaches for the degradation of MPs and bulk plastics. Before getting into the details for Fenton and Fenton-like reactions. It is important to distinguish between Fenton and Fenton-like reactions and advanced oxidation processes (AOPs), as many studies tend to use these terms interchangeably. AOP is a broad category of techniques designed to oxidize and mineralize persistent organic pollutants. It includes processes where chemical oxidants like ozone, Fenton's reagent, electrochemical or photochemical methods are applied to produce reactive oxygen species (ROS). The core principle of AOPs is the in-situ generation of highly reactive, short-lived radical species, such as ·OH, sulfate radicals ($SO_4{\cdot}^-$) or others, which are strong oxidizers and can chemically break down organic contaminants. While, Fenton reaction uses ferrous iron (Fe^{2+}) or other multivalent metal ions to activate H_2O_2 and produce ·OH or other ROSs. Detailed reaction mechanism is listed below.

Mechanism: Fenton reaction involves the reaction of Fe^{2+} with H_2O_2 to produce ·OH, which are strong oxidizers, and ferric iron (Fe^{3+}). Fe^{3+} is then reduced back to Fe^{2+} by another molecule of H_2O_2, creating a chain reaction as shown in Equation 1 and 2. The overall effect is the generation of ·OH, which are highly reactive and capable of oxidizing and degrading organic pollutants [75]. While for Fenton-like reactions, different metal catalysts, ligands, or peroxides, operating under modified conditions such as different pH or the application of light or electricity can be applied, leading to variations in the reaction mechanism and the production of various ROS. The Fenton/Fenton-like reaction belongs to one type of the AOP. In Fenton/Fenton-like oxidation systems, multivalent metals, such as Fe, Cu, Co, Mn, Ce, Ag, Cr, Ru, W, Mo, V, Ti, etc., are commonly applied catalysts which can activate H_2O_2 and generate ROS. The mechanism is through changes of low-valent metal (Mn^+) with reduction properties and high-valent metal ($M^{(n+z)+}$) with oxidation properties due to the reductant and oxidant properties of H_2O_2. Besides H_2O_2, organic peroxides (ROOH) or peroxydisulfate ($S_2O_8^{2-}$) and persulfate (HSO_5^-) can also be used. Fenton/Fenton-like reactions can be carried on in homogeneous and non-homogeneous systems. While, in terms of the driving force used, photo-, electrically-, ultrasonically-, and piezoelectrically-triggered Fenton reactions can be divided as shown in Figure 6. For detailed information for Fenton and Fenton-like reactions, including mechanism, application system, and materials, reviewer papers [76–78] can provide ample information.

$$Fe^{2+} + H_2O_2 \rightarrow Fe^{3+} + \bullet OH + OH^- \quad (1)$$

$$Fe^{3+} + H_2O_2 \rightarrow Fe^{2+} + \bullet HO_2 + H^+ \quad (2)$$

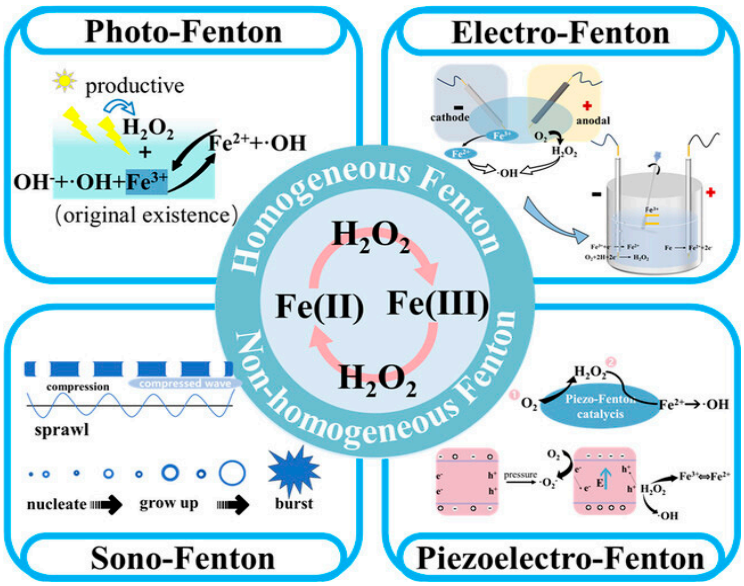

 doi:10.20944/preprints202509.1076.v1

Figure 6. Schematic illustration of MPs degradation mechanisms for different types of Fenton and Fenton-like reactions [78].

Towards a green MPs Fenton degradation, a sustainable cuttlefish bone (CFB)-supported $CoFe_2O_4$ nanoparticles has been prepared with persulfate Fenton-like strategy for the efficient degradation of PS-NPs [79]. 88.27 % removal can be done in 30 min due to fast persulfate activation through Co^{3+}/Co^{2+} redox cycle. Based on Fenton-like reaction utilizing peroxymonosulfate (PMS) as oxidant, CuMg co-doped carbonized wood sponge catalysts (CuMgCWS) with concentrated loading and dispersed distribution of Cu/Mg nanoparticles are synthesized [80]. 80 wt% selectivity for MPs to hydrocarbons and ketones can be realized due to Mg-O sites in Cu/C sponge which controlled the interfacial charge distribution and promoted adsorption and activation of PMS through Cu-centered sites. Cobalt/carbon quantum dots (Co/CQD) core-shell nanoparticles with regulated position and close intimacy are also designed for Fenton-like PP degradation [81]. Through CQD strong reduction effect accelerated Co^{2+}/Co^{3+} cycle, a significantly higher degradation activity can be realized.

Limited oxidation efficiency constrains the wide application of Fenton and Fenton like oxidation for MPs degradation. To increase the process performance, a combined Fenton reaction system is usually constructed. For instance, heterogeneous electro-Fenton (EF) PS MPs degradation processes have been demonstrated through constructing a copper-cobalt carbon aerogel (CuCo-CA) bifunctional cathode [82]. The CuCo-CA possesses H_2O_2 electro-synthesis and *in situ* activation of ·OH generation capability (without the need for external aeration) for oxidative decomposition of PS-NPs. 94.8 % of PS NPs removal efficiency can be achieved in 6 h. Similarly, a piezo-Fenton process is also developed using ferroelectric $Bi_{12}(Bi_{0.5}Fe_{0.5})O_{19.5}$ catalyst [83]. $Bi_{12}(Bi_{0.5}Fe_{0.5})O_{19.5}$ with exceptional piezoelectric properties can ensure efficient polarization under ultrasonic field to generate a substantial amount of ROSs, resulting in degradation PET-MPs via piezocatalysis/Fenton-like mechanism. 28.9 % removal rate of PET MPs can be achieved in 72 h. Besides coupling Fenton reaction with electro and ultrasonic field, a visible-light-driven photocatalysis and photothermal Fenton-like reaction has been formulated utilizing an α-Fe_2O_3 nanoflower on hierarchical TiO_2 (opal-like layer/nanotube arrays, denoted as α-Fe_2O_3/TiO_2HNTAs film) [84]. Under light initiation and photothermal effect, without external H_2O_2 input, nearly 100% degradation of 310 nm PS spheres can be obtained after 4 h at 75 °C. It is found that PS can melt at temperature much lower than its melting point in the process and TiO_2HNTAs promotes the PS degradation efficiency on α-$Fe_2O_3$is (active sites) through electrons population. Interestingly, without using a catalyst, Hu et al. [85] demonstrates that a hydrothermal-coupled Fenton reaction can achieve up to 95.9% mass loss and 75.6% mineralization of PE MPs within hours, due to synergistic thermal hydrolysis and hydroxyl radical oxidation. A summary of catalyst, reaction condition and performance for Fenton and Fenton-like MP degradation is shown in Table 5.

Table 5. Summary of catalyst, reaction condition and performance for Fenton and Fenton-like MP degradation.

Catalyst	Plastic type	Size	Mechanism	Condition	Products	Quantification method	Efficiency	Ref.
Cuttlefish Bone-Supported $CoFe_2O_4$ nanoparticles	PS	70 nm	Fenton-like	100 rpm and 25 °C, APS dosage (0.25–1.25 g/L)	NA	TOC analyzer	88.27 % removal in 30 min	[79]
CuMg co-doped carbonized wood sponge catalysts CuMgCWS	PP	NA	Electro-Fenton	Hydrothermal at 160 °C for 14 h	Hydrocarbons and ketones	Weight loss, GCMS	80 wt% selectivity to hydrocarbons and ketones	[80]
Cobalt/carbon quantum dots core-shell nanoparticles	PP	< 25μm	Fenton-like	4.0 ml of hydrogen peroxide 35% v/v	NA	Weight loss	9.6% degradation in 24 h	[81]
Copper-cobalt carbon aerogel (CuCo-CA)	PS	~119 nm	Fenton	Current: 20 mA, initial pH: 7.0, electrolyte 0.05 M	Acetophenone, benzoic acid, esters, aldehydes, and alcohols	FTIR, UV-Vis, and direct infusion MS	94.8 % removal efficiency in 6h	[82]
Ferroelectric $Bi_{12}(Bi_{0.5}Fe_{0.5})O_{19.5}$	PET	500–600 μm	Piezo-Fenton	Ultrasound treatment (40 kHz, 120 W), RT	NA	Weight loss, HPLC, LC-MS	28.9% removal rate in 72 h	[83]
α-Fe_2O_3 nanoflower on TiO_2 with a hierarchical structure	PS	310 nm	Photo-Fenton	A Hg lamp (365 nm, 0.5 W cm−2) , 75 °C	Carboxylic acids or carboxylates, CO2	1H NMR, GC	Nearly 100% degradation in 4 h at 75 °C	[84]
Zeolitic imidazolate framework@hydrogen titanate nanotubes (HTNT@ZIF-67)	Toothpaste MPs	~300 μm	Fenton	1 mL, 30% H_2O_2 addition	NA	HPLC-MS and weight loss	97% removal efficiency in 3h	[86]

 doi:10.20944/preprints202509.1076.v1

Developing Fenton like reactions coupled with other activation methods shows great promise for enhanced MP degradation due to the technology maturity, easy to scale up and low cost. However, there are many more to be studied, especially in terms of the mechanism understanding in the complicate system. As demonstrated in the recent work [87], Fenton, photo-Fenton, and Fenton-like processes show polymer-specific efficacy—some microplastics respond to light-assisted oxidation while others remain refractory. Consequently, a one-size-fits-all Fenton treatment is unlikely; a tailored or hybrid strategy matched to polymer type is preferable. Besides, MPs degradation using Fenton and Fenton like reaction are usually carried in aqueous system on a laboratory scale. Its wide application and implementation of are limited due to the long reaction time, low liquid phase degradation efficiency and the formation of secondary nanoplastics [88]. Therefore, future catalyst developments should focus on real condition related environment and more effective and faster reaction pathways.

4.3. Thermal Catalytic Process

Thermal catalytic treatment of MPs offers super-efficient way of transforming MPs into nonhazardous products (CO_2 and H_2O), value added chemicals and fuels through oxidation, pyrolysis, and reforming mechanism. With a use of catalyst, the process efficiency can be improved, especially for lowering the reaction temperature and elevating the products selectivity. With careful design of the catalysts, using composite, constructing bifunctionality, controlling structure and surface properties, enhanced MPs transformation and degradation can be realized.

Mechanism: Thermal–catalytic microplastic treatment couples heat with a solid or homogeneous catalyst to depolymerize MPs into smaller intermediates or convert them into value-added products (e.g., fuels or carbon materials). In this approach, thermal energy drives bond cleavage while the catalyst lowers activation barriers and improves selectivity, enabling effective conversion at lower temperatures than thermal cracking alone. Reported catalysts include biochar, metal-modified biochar, and Fenton-like systems, applied in both liquid- and gas-phase processes to accelerate degradation and steer product distributions.

An intensified PS MPs adsorption and pyrolysis degradation process is formulated, by modifying magnetic biochar (MBC) with Mg/Zn [89]. Through the magnetic catalyst design, the MPs and adsorbents can be easily separated through a simple magnet. What is more, MPs degradation and adsorbent regeneration can be accomplished by thermal treatment simultaneously. The authors found that Mg/Zn modification improves MPs adsorption through an increased electrostatic interaction and chemical bonding. A bimetallic Ni-Pd/TiO_2 is formulated by adding Pd into Ni [90] to increase catalyst redox properties and basic sites for MPs transformation to useful H_2 and liquid hydrocarbons. The process is based on Ni-Pd/TiO_2 as a cracking and steam reforming catalyst. At 700 °C, H_2 yield of 93% and phenol conversion of 77% can be achieved. The superior H_2 selectivity is due to the increased catalyst redox properties and basic sites introduced by Pd.

Catalytic thermal treatment is an effective way of upcycling MPs through converting them into novel carbon-based catalysts that can be used for other catalytic processes. For instance, Shengjia Ma et al. [91] turn PS MPs into a Fe/Mo doped sponge-carbon (Fe/Mo-N-C) through a one-step pyrolysis process. The prepared catalyst shows effective oxidation of 17α-ethinylestradiol (EE2). Similar work [92] has also been performed for PET MPs through controlled carbonization, resulting in a zero-valent iron loaded porous carbon catalyst that can degrade tetracycline in high efficiency. To increase the thermal catalytic oxidation process efficiency and lower the reaction temperature, a Hopcalite ($CuMnO_x$) catalyst is used and combined with dielectric barrier discharge (DBD) plasma [18], formulating a two stage reaction system for PS MPs complete degradation. In the first step, the DBD plasma generates ROS for PS-MPs degradation. While in the second stage, Hopcalite catalyst selectively converted the intermediates to CO_2 with a high efficiency of 98.4% in 60 min. By using $NiCl_2$ with HDPE, different structured carbons (core-shell carbon composites, nanosheets, and their hybrids) which show promising catalytic effect for peroxymonosulfate activation for phenol

 doi:10.20944/preprints202509.1076.v1

degradation in water [93]. The morphology and proportions of structure defective carbon can be easily controlled by tuning the $NiCl_2$ to HDPE ratio. In the process, $NiCl_2$ serves as both a catalyst and template for HDPE conversion. The working mechanism is that HDPE is firstly pyrolyzed into hydrogen and light hydrocarbons which can reduce Ni^{2+} to zero-valent Ni^0 which is the active site for light hydrocarbons conversion to carbon rich compounds.

A summary of catalyst, reaction condition and performance for thermocatalytic MP degradation is shown in Table 6. Despite the high reaction rate and efficiency of treating MPs using thermochemical methods (catalytic pyrolysis, hydrocracking, hydrogenolysis, oxidative degradation, and tandem upcycling), catalyst deactivation due to coking, active sites leaching, and sintering is still a big issue to be resolved [94]. Besides, there is also a product selectivity control challenge as varied hydrocarbon chain length with O and halogen atoms tend to be formed, impairing the value of the products. Therefore, future thermal catalysts development should focus on tackling the stability, products selectivity, and catalyst scale up issues.

Table 6. Summary of catalyst, reaction condition and performance for thermal catalytic MP degradation.

Catalyst	MP type	Size	Mechanism	Condition	Products	Quantification method	Efficiency	Ref.
Hopcalite-($CuMnO_x$)	PS	200 µm	Plasma assisted thermal oxidation	Plasma (20.6 kV, 8.6 kHz), 79% N_2 and 21% O_2	CO_2	Weight loss and Micro GC	98.7 % PS-MPs conversion to CO_2 in 60min	[18]
Mg/Zn -MBC	PS	1.0 µm	Pyrolysis	500 ◦C for 10 m	Aromatics in the range of C6-C9,	MPs weight concentration	94.81% MBC only 98.75% Mg-MBC 99.46% Zn-MBC	[89]
Anatase-Rutile Ni-Pd/TNPs	Mixed MPs made from waste plastics blending	<= 5 mm^2	Reforming and cracking	500–700 °C, N2, phenol dissolved MPs as feed	H_2 and liquid fuels	GC-MS, FTIR, GC-FID, and GC-TCD	H_2 yield (93%) and phenol conversion (77%) at 700 °C	[90]
$NiCl_2$	HDPE blended to small size	NA	Pyrolysis	800 °C, 3 h, N2	Functional carbon	TGA-DSC	33.4% carbon yield with 15:1 catalyst to HDPE ratio	[93]
Co-N/C@CeO_2 composite	PET	~4 µm	Thermal-Fenton	PMS (5 mM) + Co-N/C@CeO_2 (0.5 g/L) + H_2O_2 (1 mL), T = 55–65 °C,	HC intermediates, CO_2 + H_2O	Mass loss; GC–MS; UPLC-MS	92.3% PET MPs degradation at 55 °C with PMS + H_2O_2 (vs. 52.3% without H_2O_2)	[95]
Fe^{3+}, Al^{3+}, Cu^{2+}, Zn^{2+}	PE (spheres & fragments), PA (fibers), PP (fragments)	150–500 µm	Hydrothermal degradation	180–300 °C, 30 min, (10–85 bar)	Olefins, paraffins, ethanol, glycols; nanoplastics	Weight loss SCOD, TOC, GC–MS, Py–GC–MS, FTIR	PA: >95% in Fe^{3+}, 92% in Al^{3+} at 300 °C; PE: ~17–25%; PP: ~13% in Fe^{3+} at 300 °C;	[96]
Zeolite catalysts	PE, PP, PS, PET, PVC	Pellets (~3 mm) or powders (<1 mm)	Pyrolysis	300–600 °C, often ~500 °C, 0.1–0.8 MPa; 15–120 min;	Olefins, aromatics, gasoline/diesel paraffins, waxes, H_2, CH_4, C_2–C_4	GC–MS, TGA, FTIR;	Liquid oil yield: 80–90%;	[97]
ZnO nanoparticles (<50 nm)	PP	Macro: 100 mm^2; Micro: 25 mm^2	Thermo-photocatalytic	UV-C (254 nm, 11 W), 1–3 g/L ZnO, 35–50 °C, 6 h, air bubbling (1.6 L/min)	Nano plastic	Weight loss measurement	7.89% weight loss in 6 h	[98]
Fe-MBC	PS	100 nm	Pyrolysis	550 °C, 10 min, N_2 atmosphere	Styrene (74.6%), benzene, toluene, ethylbenzene, α-methylstyrene	UV–Vis (224 nm) for PS conc. GC–MS(initial)	Removal efficiency ≈99%	[99]

4.4. Bio and Bio-Inspired Catalysts

Biodegradation of MPs is considered as the most environmentally friendly and cost-effective degradation technology to handle environmental related MPs, due to the widespread of microorganisms and their ecosystem compatibility [100]. MP biodegradation is primarily driven by microorganisms like bacteria, fungi, and algae that secrete enzymes to break down plastic polymers into simpler compounds. The process involves biofragmentation, where enzymes cleave polymer chains, followed by assimilation and mineralization, where microorganisms further break down these fragments, eventually incorporating them into their cells or converting them into harmless byproducts like CO_2.

Mechanism: Four-stage biodegradation paradigm is usually applied for MPs—conditioning/colonization → fragmentation (oxidative/abiotic assist) → enzymatic depolymerization to oligomers/monomers → assimilation & mineralization (CO_2/H_2O, or CH_4 anaerobically)—through the use of key enzymes (e.g., PETase/MHETase, cutinases, laccases, peroxidases) and microbial taxa. MPs degradability could be affected by polymer chemistry, crystallinity, hydrophobicity, particle

 doi:10.20944/preprints202509.1076.v1

size, additives, and aging etc. [101]. More information in terms of the general methods and mechanism for microplastic degradation can be learn from the review work [102,103].

Immobilization of *Candida rugosa*-CrL enzyme in metal-organic frameworks (CrL_MOFs) is formulated for Bis-(hydroxyethyl) terephthalate (BHET) degradation [104] with increased stability and recyclability of enzyme type catalysts. Due to the MOF's adsorption capability to concentrate MPs related products, 37% of removal efficiency in 24 h can be achieved through the enzymatic degradation. Using a pre-concentration approach, hydrophilic bare Fe_3O_4 nanoaggregates are used to adsorb major MPs via hydrogen bonding [105]. Besides the adsorption, the hydrophilic Fe_3O_4 surfaces also shows a peroxidase-like nanozyme activity to degrade organic pollutants. 100 % of PP, PE, PVC, PS, and PET can be degraded through an autoclave-based heating approach. Modification of bacteria has also been conducted to improve MPs' degradation performance. A *Shewanella putrefaciens 200* Fe-reducing bacteria is prepared taking advantage of microbially driven Fenton reaction for PS-MP degradation [106]. ·OH produced by the microbially driven Fenton reaction shows a PS-MPs degradation of 6.1 ± 0.6% weight loss in 14-day. The authors found that ·OH-induced oxidative could damage the microorganisms, affecting continuous ·OH production. Therefore, timely replenishment of organic carbon sources is the key to sustain a reproduction of microorganisms. In another work, an engineered bacterium through rational design of biological manganese oxides (BMO mediated by SDE-PsLAC) is used for PE MP degradation [107]. SDE-BMO shows significantly enhanced PE MPs catalytic degradation due to weakened MPEs inertia. The improvement of microbial MP degradation efficiency through metal ions is also observed by Xionge Li et al. [108]. Durign the study, they found that PE MPs biodegradation by marine sediment bacteria tends to be enhanced under iron-enhanced conditions. The enhancement is due to the generation of multiple oxygen-containing functional groups resulting from the addition of Fe^{3+}. Besides bacterial modification approach, Mn-doped iron phosphate (LFMP) bio-inspired nanozymes have also been synthesized for PE and PP degradation [109]. Through Mn^{2+} doping, expanded LFP lattice structure with narrowed bandgap can be realized, enhancing Li^+ migration rates which increases the peroxidase-like MPs degradation activity.

Bio-Fenton approach is an emerging method for microplastic degradation which combines Fenton oxidation and microorganisms. By combining MnO_2/g-C_3N_4/fly ash (MCNF) micromotors induced Fenton reaction and *B. subtilis* Microbial degradation, 60% of PS degradation within 24 days and 66% of PE degradation within 50 days are realized [110]. A clear elevated degradation process can be observed as shown in Figure 7. The bio-Fenton method shows much better performance compared to the sole use of Fenton reaction or microbial degradation. The authors claimed that the improved degradation performance is ascribed to the self-propelled motion of MCNF micromotors which improves the mass transfer efficiency of the Fenton reaction.

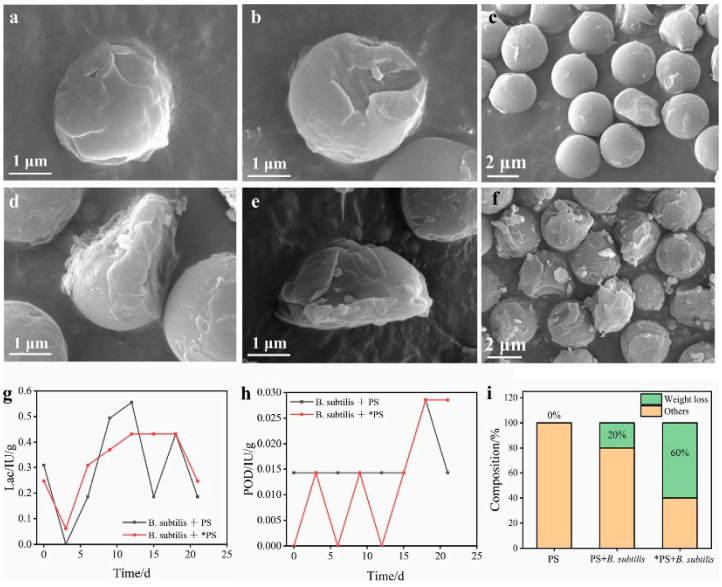

 doi:10.20944/preprints202509.1076.v1

Figure 7. (a–c) SEM images of PS degradation using B. subtilis soil for 24 days. (d–f) SEM images of PS degradation through Fenton reaction pretreatment and B. subtilis for 24 days. Enzyme activity of (g) Laccase and (h) Peroxidase concentration using different catalysts combination, and (i) Weight loss of PS using different catalysts combination (*PS indicates Fenton reaction-pretreated PS) [110].

Table 7. Summary of catalyst, reaction condition and performance for biological catalytic MP degradation.

Catalyst	Plastic type	Size	Condition	Products	Quantification method	Efficiency	Ref.
Candida rugosa lipase (CrL) immobilization in metal-organic frameworks (CrL_MOFs)	Bis-(hydroxyethyl) terephthalate (BHET) as model compound	NA	Water, 25 °C, 1 bar	H2BDC	High performance liquid chromatography (HPLC)	37 %, 24 h,3 mg of degraded BHET per g of enzyme	[104]
Hydrophilic bare Fe_3O_4 nanoaggregates	HDPE, PP, PVC, PS, and PET	20-800 µm	130-260 °C, autoclave	NA	UV-vis and weight measuring	100 % degradation close to their melting temperature	[105]
Shewanella putrefaciens 200	PS	1.20 -1.30 mm	25 °C and PH: 7.0 in water solution	Benzene ring derivatives	Weight loss was measured by an analytical balance	Weight loss of 6.1 ± 0.6% in 14 days	[106]
Manganese oxide free radicals modified *SDE-PsLAC, E. coli BL21*	PE	500–1500 µm	37 °C or 15 °C for 192h	Aromatics, aliphatics, alcohols, and esters	Weight loss	91.2 % at 37 °C and 52.4 % at 15 °C within 192 h	[107]
Iron-enhanced microbiota	PE	3–5 mm^2 piece from commerical plastic bag	30 to 60 days of cultivation at 37 °C	Heneicosane, octadecane, pentadecane, and 4,6-dimethyl dodecane	Weight loss	12.38% weight loss in 60 days compared to 10.44% for non iron added samples	[108]
MnO_2/g-C_3N_4/fly ash (MCNF)	PS, PE	5 µm	RT with H_2O_2 addition	NA	Weight loss	PS degradation 60% in 24 days; 66% PE degradation in 50 days	[110]
Engineered S. pavanii with *DuraPETase*	PET	500 µm	30 °C and 150 rpm	TPA, MHET, BHET	HPLC	38.04µM products generation after 30-day incubation at 30 °C	[111]
Mn-doped iron phosphate(LFMP)	Polyamide 6, HDPE, and pp	0.5 to 4.5 mm	25 °C or 180 °C for 8h in autoclave	CO_2, H_2O_2, and inorganic small molecules	Weight loss	91.5% at 180 °C for 8h. 3 times higher than that no doped LFP	[112]

A summary of catalyst, reaction condition and performance for biological catalytic MP degradation is shown in Table 7. Biodegradation offers significant advantages in terms sustainability, circular economies under mild conditions, however it faces challenges such as slow reaction rate, susceptible to environmental changes, and complicated reaction mechanism. Research is ongoing to enhance these processes through techniques like protein engineering and strain breeding, aiming to improve the efficiency and environmental safety of MP biodegradation. MPs biodegradation is a slow process which can take days and months to proceed [113], lacking a capability to effectively remove the much-accumulated environmental MPs. Therefore, formulating eco-friendly solutions to accelerate MPs degradation is the key.

4.5. Electrocatalysts

Electrochemical catalyst systems are increasingly important for MP treatment because they generate oxidants and reductants in situ, eliminating bulk chemical dosing and minimizing secondary pollution. Their activity is readily tuned by potential, electrode composition, and electrolyte, enabling modular reactors that scale from lab cells to flow systems and that operate in diverse matrices (including salted and fresh waters). Beyond simply degrading stubborn polymers (PE, PET, PP, PS) and halogenated plastics (PVC), advanced paired electrochemical systems can upcycle plastic-derived intermediates into value-added products (e.g., formate, carboxylic acid, and etc.) while simultaneously producing H_2, offering an efficient strategy to integrate renewable electricity and realize a green pathway.

Mechanism: The electrochemical degradation of MPs can be divided into indirect oxidation and direct oxidation. For indirect oxidation, ROS is generated in the bulk solution or at the electrode surface. Then, these highly unstable and non-selective radicals attack and break the strong bonds within the MPs. While, for direct oxidation, MPs can directly interact with the anode surface, leading to a direct electron transfer reaction. Regardless of the initiation pathway (indirect or direct oxidation), the degradation of MPs follows a general process of polymer attack and fragmentation.

Mao et al. developed a sustainable electrocatalytic upcycling method to convert PET microplastics into value-added products (H_2, TPA and formate) through a two-stage process using

 doi:10.20944/preprints202509.1076.v1

$Mn_{0.1}Ni_{0.9}Co_2O_4$-δ rod-shaped fiber spinel catalyst [114]. In the first stage, PET MPs (particle size <500 μm) are hydrolyzed with potassium hydroxide (KOH) to release terephthalic acid (TPA) and ethylene glycol (EG). In the second stage, the extracted EG is used as the anolyte and undergoes anodic oxidation on the $Mn_{0.1}Ni_{0.9}Co_2O_4$-δ rod-shaped fiber spinel catalyst, achieving formate production with over 95% Faradaic efficiency at 1.42 V vs RHE, while the cathode simultaneously facilitates hydrogen evolution, thereby producing both clean energy and valuable chemicals from plastic waste. The superior performance is due to Mn doping which changes the electronic structure, reducing the lattice oxygen oxidation in the $NiCo_2O_4$ spinel oxide as OER electrocatalysts. Doping Mn, Co, or Ru as an intermediate layer between titanium (Ti) substrate and La-Sb-SnO_2 active layer has also been conducted to improve lifespan of the electrode for PS MPs electrochemical oxidation [115]. With Co dopant as the interlayer, PS-degradation performance (28% mass loss in 3h) is 4.54× vs no interlayer, 2.38× vs Ru, and 1.19× vs Mn dopant counter parts. What is more, 5 times prolonged lifespan can be achieved using Ti/La/Co/-Sb-SnO_2 anode. Similar work has been conducted by the same group using La as a dopant for Ti/Sb-SnO_2 electrode [116]. The results show that La promoted the formation of ·OH radicals and increased the PS MPs degradation efficiency by 77% compared to Ti/Sb-SnO_2 only. Metal oxide has also been used as dopant to improve the electrochemical oxidation performance. CeO_2-doped PbO_2 anode has been prepared to for PVC MPs degradation [117]. Compared with undoped PbO_2, the CeO_2–PbO_2 electrode shows mass loss of PVC MPs and clear surface damage (cracks, reduced particle size) during treatment. The system achieves about 39% PVC weight loss in 6 h, attributed to persulfate/·OH generated from the sulfate electrolyte and high anode potential. Through CeO_2 doping, β-PbO_2 grains are refined, resulting in improved grain arrangement, increased amount of active site.

Ma et al. designed a novel Ni_3N/W_5N_4 Janus nanostructure with a seamless heterointerface, synthesized via a transition-metal nitride–induced growth method [118]. The seamless interface can enable synergistic charge redistribution, lower the reaction energy barrier, and facilitate efficient electron transfer. Within this heterointerface, Ni_3N supplies abundant active sites for the hydrogen evolution reaction (HER), while W_5N_4 enhances electrical conductivity and provides strong stability under harsh seawater conditions. Moreover, the junction between Ni and W nitrides effectively modulates the d-band center, thereby optimizing the adsorption and desorption of reaction intermediates and contributing to the overall catalytic efficiency. Besides, the Janus architecture exhibits superb hydrophilicity and an interface synergy that grants Pt-like performance for the hydrogen evolution reaction (HER), with remarkable stability (~300 hours) even under industrial current densities. Simultaneously, this catalyst drives the electroreforming of MPs in seawater, enabling the production of formic acid with ~85% Faradaic efficiency at an ultralow overpotential of 1.33 V.

Defect engineering, including heteroatom doping, vacancies, edge/planar defects, and nanoarchitecture control has been extensively used to tune 2D graphitic carbon nitride (g-C_3N_4) for enhanced light absorption, charge separation, redox kinetics, and surface adsorption of MPs waste remediation [119]. Through the approach, Yuan Wang and colleagues [120] report the development of a cost-effective, self-supporting electrode composed of vacancy-rich NiFe layered double hydroxide (NiFe_V-LDH) nanoarrays grown in situ on carbon paper, designed for electro-Fenton degradation of PVC microplastics. This electrode exhibits high selectivity (~76%) for generating H_2O_2. Density functional theory (DFT) calculations demonstrate that oxygen vacancies significantly lower the energy barrier for H_2O_2 desorption, enhancing catalytic performance. The optimized system leverages both direct cathodic reduction of PVC and ·OH-mediated oxidation, driven by the electro-Fenton process. A summary of catalyst, reaction condition and performance for electro-catalytic MP degradation is shown in Table 8. Despite showing advantages for value added chemical production for MPs degradation, electrochemical approaches still suffer from many challenges, including incomplete MPs degradation, high energy consumption, low energy efficiency, and reaction system associated high costs.

Table 8. Summary of catalyst, reaction condition and performance for electro-catalytic MP degradation.

Catalyst	Plastic type	Size	Condition	Products	Quantification method	Efficiency	Ref.
$Mn_{0.1}Ni_{0.9}Co_2O_4$-δ rod-shaped fiber (RSF) spinel catalyst	PET	<500 μm	5 mV s−1, 1 M KOH (pH = 14), 0.17 M ethylene glycol	H_2 and formate	NMR spectrometer	EG to formate with >95% Faradaic efficiency at 1.42 V vs RHE	[114]
Ti/La/Co-Sb-SnO_2 anode	PS	150 μm	0.5mol/L H_2SO_4 LSV:scanning rate: 1.0 mV s^{-1}, V: 0 to 2.5 V.	Alcohols, monocarboxylic acids, dicarboxylic acids, esters, ethers, and aldehydes	Weighing method and PY-GCMS	28% removal in 3 h	[115]
Ni_3N/W_5N_4 janus	PET flakes	<500 μm	Scan rate of 5 mV s^{-1}	H_2 and HCOOH	NMR spectrometer	~85% Faradaic efficiency	[118]
Vacancy-rich NiFe-LDH/carbon paper	PVC	74–147 μm	10 to 100 mV s^{-1}	H_2O_2	Ion Chromatography (IC) and GC–MS	~76% selectivity for H_2O_2	[120]
CeO_2-modified PbO_2 anode	PVC	NA	T:20–100 °C, 10–60 mA/cm^2, pH (3–11), PVC-MPs (50–150 mg/L), and Na_2SO_4 10–90 mM	H_2O and CO_2	Weight loss and HPLC-MS	38.67% weight loss in 6 h. 16.67% increase compared to pristine PbO_2 anode	[117]

 doi:10.20944/preprints202509.1076.v1

4.6. Hybrid Catalysts Coupling Different Reaction Pathways

Hybrid catalyst systems have emerged as a promising strategy for the elimination of microplastics, as they integrate two or more catalytic mechanisms to enhance degradation efficiency. For example, the combination of photocatalysts and enzymatic catalysts can accelerate the breakdown of polymers while simultaneously improving conversion rates into environmentally benign byproducts. Compared with conventional single-catalyst approaches, hybrid systems offer distinct advantages, including higher degradation efficiency, faster reaction kinetics, and greater overall effectiveness, thereby positioning them as a sustainable and advanced solution for addressing MP pollution [121].

A MPs to CH_4 process with nearly 100% of CH_4 selectivity is demonstrated in the work of Ye et al. [122]. M. b-CDPCN biohybrid catalysts are constructed by assembling Methanosarcina barkeri (M. b) and carbon dot-functionalized polymeric carbon nitrides (CDPCN). A maximum CH_4 yield of 7.24±0.40 mmol g^{-1} can be achieved with the *M. b*-CDPCN biohybrids, which is 34.5-fold and 16.8-fold higher than *M. b*-PCN and *M. b*-CDPCN with cysteine respectively. The methanogen-semiconductor biohybrids in the work use MPs as an electron and energy source for CH_4 generation. Both the photooxidation methanogenesis (i.e., pyruvate/acetate-to-CH_4 conversion by reactive species) and photoreduction methanogenesis (i.e., CO_2-to-CH_4 conversion by photoexcited electrons) work together to contribute to the high CH_4 yield and selectivity.

Through integration of carbocatalytic oxidation and hydrothermal (HT) hydrolysis with sulfate radical, a magnetic N-doped nanocarbon springs is formulated [123] to degrade MPs. Results show that the magnetic nanohybrids can effectively active peroxymonosulfate (PMS) to generate highly oxidizing radicals for MPs degradation under hydrothermal conditions. 40 wt% of MPs removals can be achieved in 8 h through the hydrothermal assisted catalytic PMS activation approach (using the N-doped nanocarbon springs) compared to 5% and 17% MPs degradation without catalyst and PMS only conditions. What is more, through toxicity tests, the organic intermediates generated from the formulated MPs degradation route are proven to be environmentally benign and can be used as a carbon source for algae growth, indicating a green way for water environment MPs handling. Hydrothermal-assisted Fenton-like reaction is also applied to convert ultrahigh-molecular-weight polyethylene (UHMWPE) MPs into carboxylic acids and H_2 [21]. To achieve the goal, hierarchical porous carbon nitride supported single-atom iron (FeSA-hCN) catalyzes have been prepared by formulating a tandem MP degradation–hydrogen evolution reaction. Near-total degradation of ultrahigh-molecular-weight polyethylene into C_3–C_{20} organics, with 64% selectivity toward carboxylic acids under neutral pH and hydrogen production at ~42 μmol/h under illumination can be achieved. By coupling Fenton-like oxidative degradation of MPs into electron-donating intermediates with photocatalytic H_2 evolution, both pollutant breakdown and clean energy production in a single FeSA-hCN catalyst can be realized.

In Miao et al. work [124], an innovative electro-Fenton-like (EF-like) technology is designed to degrade PVC MPs in aqueous environment by employing a TiO_2/graphite (TiO_2/C) cathode. The system can simultaneously promote cathodic reductive dechlorination and ·OH oxidation, enabling effective degradation. Using the idea of process intensification and fabricating heterogeneous materials to modulate the interfacial electronic structure, ternary heterogeneous interpenetrating catalysts $Fe_{1-x}S$/$FeMoO_4$/MoS_2(Mo_5Fe_5) are also prepared to enhance MPs degradation through a piezo-photocatalytic approach [125]. Under sonication and simulated light conditions, 58.46 % of PS-MPs can be degraded in 30 h. The superior performance is due to the ternary heterogeneous structure where piezoelectric response and illumination both favor the generation of H_2O_2, leading to the rapid activation of ROS for MPs degradation.

An innovative photo-electrocatalytic–biocatalytic hybrid system that transforms real-world PET MPs into value-added chemicals using solar energy has also been formulated [126]. By improving charge transport, suppressing electron–hole recombination, and lowering reaction barriers through Zr doping, the process begins with a Zr-doped hematite (α-Fe_2O_3) photoanode, which extracts

 doi:10.20944/preprints202509.1076.v1

electrons from hydrolyzed PET solutions derived from post-consumer plastic waste. These electrons are transferred to a carbon-based cathode, where they activate various redox enzymes to catalyze organic transformations such as C–H oxyfunctionalization, C=O amination, and asymmetric C=C hydrogenation.

Feng and co-workers [127] design a CoNi-alloy catalyst anchored on carbon nanocages and interconnected by CNTs, then surface fluorinated using a solvent-free CF_4 plasma treatment. The F-functionalized heterostructure shows high activity and durability for seawater electrolysis, enabling a paired system where the anode electro-oxidizes PET MPs to value-added products (e.g., formate) while the cathode produces H_2 with Pt-like HER performance. The hollow 1D/3D architecture, Co–Ni synergy, and reconstructable metal–F bonds in alkaline media enhance charge transfer and reaction kinetics. What is more, the proposed coupling strategy can have a potential saving of 165 mV at a current density of 10 mA cm^{-2}. To better illustrate, Figure 8 showcases some of the hybrid catalysts design strategies.

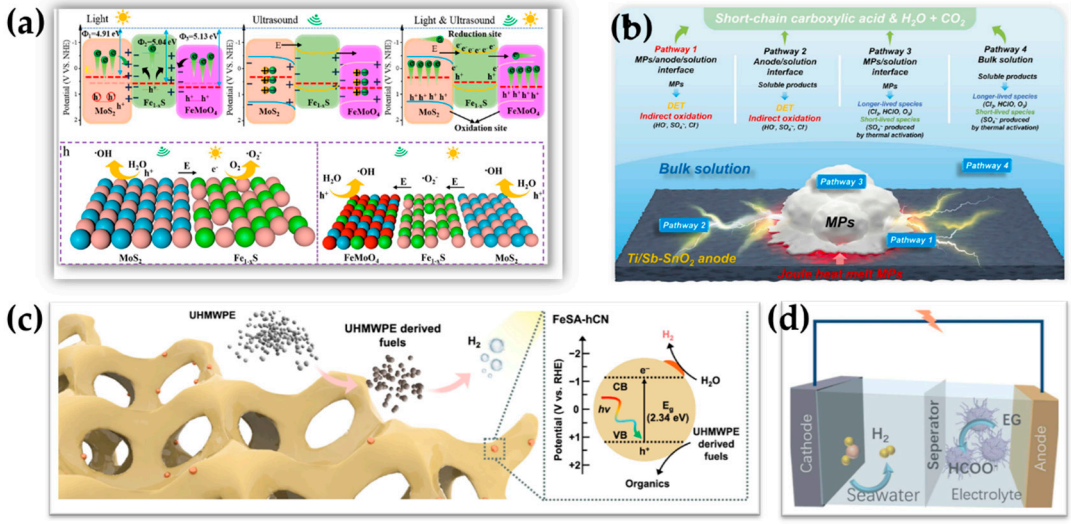

Figure 8. Hybrid catalyst design strategy illustration coupling different reaction mechanisms (a) Piezo-photocatalytic enhanced microplastic degradation [125]; (b) Joule heat assisting electrochemical degradation [113]; (c) Tandem MP degradation and H_2 production [21], and (d) H_2 evolution coupled with microplastic upcycling [127].

Besides the aforementioned methods, a novel Joule-heat–assisted electrochemical strategy is also developed by using a hybrid membrane consisting of a Sb-SnO_2 coated titanium mesh (Ti/Sb-SnO_2) and a carbon felt (as assistant) as anode [128]. In the specially designed reactor, PE MPs can be captured by anode, being softened or even melted by the interface Joule heat which enables a direct electron transfer from anode to MPs and make the most use of short-lived active species. Above 99 % of PE MPs removal efficiency can be achieved within 6 h without nanoplastics generation and chlorinated compounds. A summary of the novel catalysts developed for hybrid approach MPs degradation is shown in Table 9. Hybrid MPs degradation approaches show great promise in terms of realizing fast reaction rate and efficient material utilization. While, there are still more to be conducted, especially for accomplishing a robust and complicated system design. In this regards, a stable and active catalyst is the key.

For a more detailed literature summary for catalysts used for microplastics degradation, the following review papers [121,129–131] can be referred within which [129] focuses on chemical catalytic processes. [130] stresses on biocatalytic approaches. [121] specifies on MPs catalytic removal in water body. While, more information in terms of the general methods and mechanism for MP degradation can be found in the review work [131].

Table 9. Summary of catalyst, reaction condition and performance for hybrid catalytic MP degradation.

Catalyst	Plastic type	Mechanism	Size	Condition	Products	Quantification method	Efficiency	Ref.
FeSA-hCN (single-atom Fe on porous carbon nitride)	UHMWPE	Tandem MP degradation + H_2 evolution	< 180 μm	Simulated solar irradiation in aqueous suspension, pH 7	64% carboxylic acid selec; H_2: 42 μmol/h	Mass loss, HPLC	Near 100% PE degradation	[21]
TiO_2/graphite (TiO_2/C) cathode	PVC	Electro-Fenton	74–147 μm	−0.7 V vs Ag/AgCl using Na_2SO_4 as supporting electrolyte	CO_2, H_2O, and Cl^-	Dechlorination efficiency through ion chromatography	~75% dechlorination efficiency in 6h	[117]
Methanosarcina barkeri (M. b) and carbon dot-functionalized polymeric carbon nitrides	Poly(lactic acid), PE, PS, and PUR	Photo-biological	≤0.04 cm^2	395±5 nm ultraviolet,35±2 °C	100 % CH_4	NA	CH_4 yield 7.24±0.40 mmol g^{-1}	[122]
Magnetic N-doped nanocarbon springs	MPs from cosmetic pastes	Integrated carbocatalytic oxidation and hydrothermal (HT)	>=0.45 μm	Peroxymonosulfate (PMS) added in a autoclave with water	CO_2 and H_2O	Filtration through a 0.45-μm membrane. Mass loss measurement and HPLC	44% of MPs decompositions in 8h	[123]
$Fe_{1-x}S$/$FeMoO_4$/ MoS_2	PS	Piezo-photo-Fenton	0.55-12.5 μm	Ultrasonic cleaner (at 120 W, 40 kHz) equipped with LED irradiation (24 W) at RT	Benzoic acid and phenylacetic acid	Centrifugation for calculating the weight loss	58.46 % of PS-MPs in 30h	[125]
Zr-doped hematite (α-Fe_2O_3) photoanode	PET	Photo-biological	<2 mm	A mixed condition	Formate and acetate	Quantitative ^1H NMR and HPLC	High faradaic efficiency (>90%)	[126]
F-functionalized CoNi-alloy catalyst	PET	Binfunctional	NA	50 to 300 mV s-1	H_2 and formate	^1H NMR	90.7% faradaic efficiency at 1.48 V	[127]
Ti/Sb-SnO_2 and carbon felt	PE, PP, PS, PVC, PLA, and PET	Thermal-electro	~400 μm	20 mA·cm^{-2} current density, Na_2SO_4 electrolyte	Oxygen-containing species, H_2O and CO_2	Weight loss and GC/MS	99 % degradation of PE MPs in 6 h	[128]

 doi:10.20944/preprints202509.1076.v1

In summary, depending on the targeted products, MPs degradation can proceed either through complete mineralization into harmless end products or through upcycling into value-added chemicals and fuels. Compared to mineralization, upcycling offers greater advantages by enabling resource recovery, promoting greener production pathways, and contributing to the development of a circular economy. Meanwhile, it also encompasses significant technical and logistical challenges across collection, processing, and end-use application. The initial obstacle involves efficient collection and removal, as MPs are dispersed across aquatic, terrestrial, and atmospheric environments, with diverse polymer compositions, particle sizes, and inclusion of other organic components that are extremely challenging to achieve a high separation efficiency [132]. Conventional filtration and sedimentation techniques often struggle with high energy demand and limited scalability, while advanced approaches such as membrane technologies, magnetic separation, or coagulation-flocculation require further optimization for large-scale deployment. Following recovery, heterogeneity in polymer type, surface oxidation, and the presence of additives or adsorbed pollutants complicate standardized upcycling pathways. Thermal, catalytic, and biological conversion strategies offer potential for transforming MPs into fuels, carbonaceous materials, or chemical precursors; however, these methods face barriers related to energy intensity, catalyst deactivation, and process integration. Besides the advanced catalyst development, logistically, the establishment of reliable supply chains for MP feedstocks remains underdeveloped, as most recovery efforts are fragmented and localized. To realize a commercial-scale upcycling, a consistent feedstock quality that can align with regulatory frameworks is a must. Therefore, addressing these challenges requires coordinated strategies that link recovery technologies with scalable conversion processes and harmonized policy frameworks to facilitate sustainable MP valorization.

5. Challenges and Future Opportunities for Catalytic Microplastic Degradation and Upcycling

To mitigate MPs pollution in the current ecosystem, strategies can be developed from two ends, cut the input or increase the output. Cut the input can include end-of-pipe (EOP) treatment and cleaner production (CP). The EOP treatment which is also called “pollute first, treat later”, refers to technologies and practices used to remove pollutants from waste streams after they have been generated, typically before discharge into the environment [133]. While, CP requires development of degradable and environmentally friendly plastics alternatives, limiting the generation of pollution at the source. Considering the early stage of the degradable plastics development and matureness of fossil fuel-based plastics, complete blocking and controlling plastic pollution from the source will not be seen in the near future. Therefore, it is vital to develop clean and green technologies to collect and degrade MPs existing in the environment.

As summarized in the work, MPs degradation could be achieved through photocatalytic, advanced oxidation, electrochemical, thermal, biological, and hybrid processes as shown in Figure 8. Photocatalytic and biological degradation routes provide a green and sustainable way to mitigate MP pollutions. However, they suffer from low process efficiency, low carbon recyclability, long degradation time and susceptible to environmental conditions. AOPs provide an effective and fast elimination way of breaking down MP molecular chains into benign substances through strong, non-selective free radicals. While, the process has limited effectiveness and low efficiency at laboratory scale. Besides, nanoplastics or other toxic byproducts tend to be generated. In terms of efficiency, thermal catalytic route is promising. In exchange, it is also an energy intensive process. Based on current research, hybrid approaches integrating advantages of different catalytic pathways seems to be a promising way out for improved energy and material utilization efficiency.

 doi:10.20944/preprints202509.1076.v1

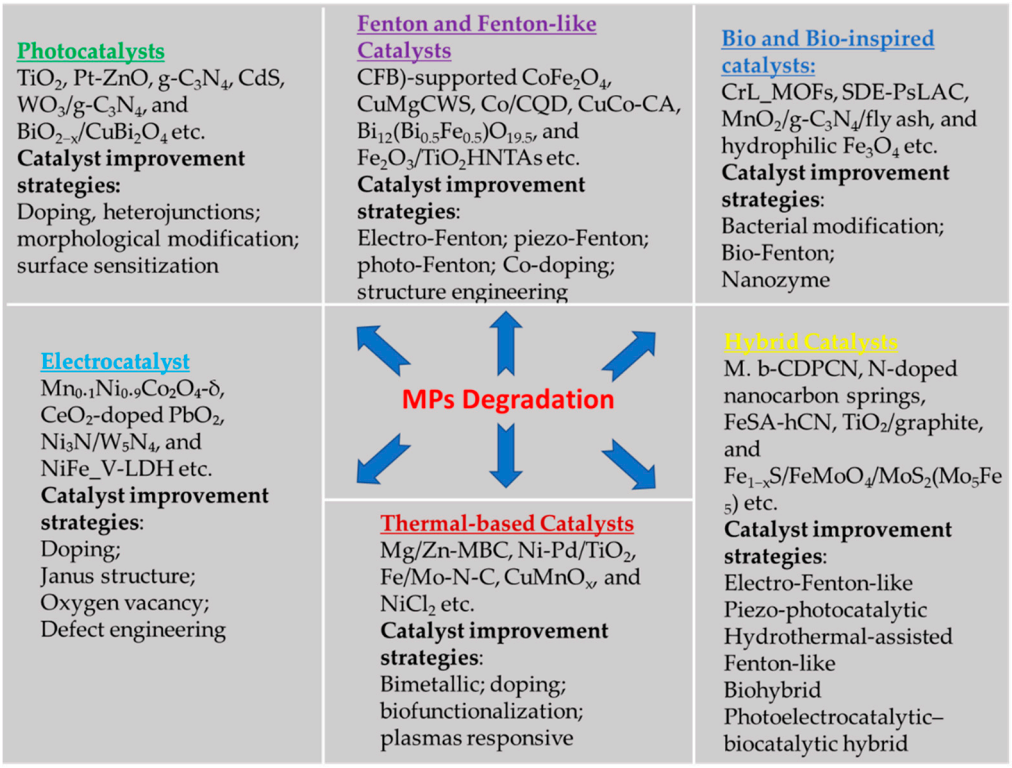

Figure 9. Summary of different types of catalysts and the catalyst activity enhancement methods used for MPs degradation.

The main challenges of current MPs degradation process include many aspects from MPs collection, quantification, identification, processing to degradation products. For instance, it is easy to tackle industrially produced MPs with high abundance and purity. While, it is extremely challenging to handle and process 'environmentally relevant microplastic' which refers to the plastic particles found in nature, including in the human diet. These differ substantially from the virgin plastic particles 'from the shelf' that are used in many laboratory experiments [134]. Not only it is challenging to collect those MPs, but also challenging for catalytic process development and performance evaluation. Besides, unsatisfying degradation performance including reaction rate, products selectivity, catalyst activity and recyclability, active sites leaching and recyclability represents another big challenge. What is more, there is a lack of standard characterization metrics (mass loss, CO_2 evolution, TOC, FTIR/Raman, GPC/SEC, SEM/AFM) and cautions about inconsistent protocols that complicate cross-study comparisons, resulting a scattered and chaotic research results. Finally, secondary pollutions caused by MPs degradation products can be a huge issue. Despite gaining increased attention, most of the studies available lack of systematic and long-term study for the effect of products from MPs degradation on human and living organisms in the ecosystem, leaving some claimed green and sustainable processes questionable.

Therefore, future directions should be focus on catalyst development toward improved reaction rate, products selectivity, energy and material utilization efficiency based on green and sustainable materials; formulated intensified catalytic processes coupling advantages from thermal, electrical, biological, and photocatalytic approaches; building modeling tools to predict and identify possible methods and materials for MPs treatment; collecting experimental and inventory data, such as MPs biodistribution, toxicity study, and life-cycle assessment [135] and make modeling and mathematical simulation to guide MPs treatment [136], and finally turn the lab-scale catalytic strategies through scale up for practical, real-world applications, addressing issues like cost, energy consumption, and long-term performance under various environmental conditions.

Author Contributions: The authors confirm contribution to the paper as follows: Review paper structure formulation, topic pick, literature search, data analysis and summary, and draft manuscript preparation: C.Z.; literature collection, analysis and draft manuscript preparation: G.Z; manuscript editing, review, and finalization: P.G. All authors have read and agreed to the published version of the manuscript.

Funding: This research received no external funding.

Data Availability Statement: No new data were created.

Acknowledgments: We would like to express our thanks to the financial support from the National Oceanic and Atmospheric Administration (NOAA) through the University of Alabama (Award NO.: NA24OARX417C0421-T1-01), and the support from National Institute of Standards and Technology (NIST) through 3D Array Technology LLC (3DAT, co-founded by P.-X.G.) with an Award NO.: 70NANB22H118.

Conflicts of Interest: The authors declare no conflicts of interest.

References

1. Thompson, R.C.; Olsen, Y.; Mitchell, R.P.; Davis, A.; Rowland, S.J.; John, A.W.G.; McGonigle, D.; Russell, A.E. Lost at Sea: Where Is All the Plastic? *Science (1979)* **2004**, *304*, 838–838. https://doi.org/10.1126/science.1094559.
2. Mohamed Nor, N.H.; Kooi, M.; Diepens, N.J.; Koelmans, A.A. Lifetime Accumulation of Microplastic in Children and Adults. *Environ Sci Technol* **2021**, *55*, 5084–5096. https://doi.org/10.1021/acs.est.0c07384.
3. Thompson, R.C.; Courtene-Jones, W.; Boucher, J.; Pahl, S.; Raubenheimer, K.; Koelmans, A.A. Twenty Years of Microplastic Pollution Research—What Have We Learned? *Science (1979)* **2024**, *386*. https://doi.org/10.1126/science.adl2746.
4. Salahuddin, U.; Sun, J.; Zhu, C.; Wu, M.; Zhao, B.; Gao, P. Plastic Recycling: A Review on Life Cycle, Methods, Misconceptions, and Techno-Economic Analysis. *Adv Sustain Syst* **2023**, *7*. https://doi.org/10.1002/adsu.202200471.
5. Sutkar, P.R.; Gadewar, R.D.; Dhulap, V.P. Recent Trends in Degradation of Microplastics in the Environment: A State-of-the-Art Review. *Journal of Hazardous Materials Advances* **2023**, *11*, 100343. https://doi.org/10.1016/j.hazadv.2023.100343.
6. Puteri, M.N.; Gew, L.T.; Ong, H.C.; Ming, L.C. Technologies to Eliminate Microplastic from Water: Current Approaches and Future Prospects. *Environ Int* **2025**, *199*, 109397. https://doi.org/10.1016/j.envint.2025.109397.
7. Welden, N.A.; Lusher, A. Microplastics. In *Plastic Waste and Recycling*; Elsevier, 2020; pp. 223–249.
8. Bermúdez, J.R.; Swarzenski, P.W. A Microplastic Size Classification Scheme Aligned with Universal Plankton Survey Methods. *MethodsX* **2021**, *8*, 101516. https://doi.org/10.1016/j.mex.2021.101516.
9. Frias, J.P.G.L.; Nash, R. Microplastics: Finding a Consensus on the Definition. *Mar Pollut Bull* **2019**, *138*, 145–147. https://doi.org/10.1016/j.marpolbul.2018.11.022.
10. Efimova, I.; Bagaeva, M.; Bagaev, A.; Kileso, A.; Chubarenko, I.P. Secondary Microplastics Generation in the Sea Swash Zone With Coarse Bottom Sediments: Laboratory Experiments. *Front Mar Sci* **2018**, *5*. https://doi.org/10.3389/fmars.2018.00313.
11. Gopalakrishnan, K.K.; Sivakumar, R.; Kashian, D. The Microplastics Cycle: An In-Depth Look at a Complex Topic. *Applied Sciences* **2023**, *13*, 10999. https://doi.org/10.3390/app131910999.
12. Hale, R.C.; Seeley, M.E.; La Guardia, M.J.; Mai, L.; Zeng, E.Y. A Global Perspective on Microplastics. *J Geophys Res Oceans* **2020**, *125*. https://doi.org/10.1029/2018JC014719.
13. Mattsson, K.; Johnson, E. V.; Malmendal, A.; Linse, S.; Hansson, L.-A.; Cedervall, T. Brain Damage and Behavioural Disorders in Fish Induced by Plastic Nanoparticles Delivered through the Food Chain. *Sci Rep* **2017**, *7*, 11452. https://doi.org/10.1038/s41598-017-10813-0.
14. Tiwari, M.; Rathod, T.D.; Ajmal, P.Y.; Bhangare, R.C.; Sahu, S.K. Distribution and Characterization of Microplastics in Beach Sand from Three Different Indian Coastal Environments. *Mar Pollut Bull* **2019**, *140*, 262–273. https://doi.org/10.1016/j.marpolbul.2019.01.055.

 doi:10.20944/preprints202509.1076.v1

15. Nobre, C.R.; Santana, M.F.M.; Maluf, A.; Cortez, F.S.; Cesar, A.; Pereira, C.D.S.; Turra, A. Assessment of Microplastic Toxicity to Embryonic Development of the Sea Urchin Lytechinus Variegatus (Echinodermata: Echinoidea). *Mar Pollut Bull* **2015**, *92*, 99–104. https://doi.org/10.1016/j.marpolbul.2014.12.050.
16. Ali, S.S.; Alsharbaty, M.H.M.; Al-Tohamy, R.; Khalil, M.A.; Schagerl, M.; Al-Zahrani, M.; Sun, J. Microplastics as an Emerging Potential Threat: Toxicity, Life Cycle Assessment, and Management. *Toxics* **2024**, *12*, 909. https://doi.org/10.3390/toxics12120909.
17. Chamas, A.; Moon, H.; Zheng, J.; Qiu, Y.; Tabassum, T.; Jang, J.H.; Abu-Omar, M.; Scott, S.L.; Suh, S. Degradation Rates of Plastics in the Environment. *ACS Sustain Chem Eng* **2020**, *8*, 3494–3511. https://doi.org/10.1021/acssuschemeng.9b06635.
18. Sima, J.; Song, J.; Du, X.; Lou, F.; Zhu, Y.; Lei, J.; Huang, Q. Complete Degradation of Polystyrene Microplastics through Non-Thermal Plasma-Assisted Catalytic Oxidation. *J Hazard Mater* **2024**, *480*, 136313. https://doi.org/10.1016/j.jhazmat.2024.136313.
19. Zhang, A.; Hou, Y.; Wang, Y.; Wang, Q.; Shan, X.; Liu, J. Highly Efficient Low-Temperature Biodegradation of Polyethylene Microplastics by Using Cold-Active Laccase Cell-Surface Display System. *Bioresour Technol* **2023**, *382*, 129164. https://doi.org/10.1016/j.biortech.2023.129164.
20. Uheida, A.; Mejía, H.G.; Abdel-Rehim, M.; Hamd, W.; Dutta, J. Visible Light Photocatalytic Degradation of Polypropylene Microplastics in a Continuous Water Flow System. *J Hazard Mater* **2021**, *406*, 124299. https://doi.org/10.1016/j.jhazmat.2020.124299.
21. Lin, J.; Hu, K.; Wang, Y.; Tian, W.; Hall, T.; Duan, X.; Sun, H.; Zhang, H.; Cortés, E.; Wang, S. Tandem Microplastic Degradation and Hydrogen Production by Hierarchical Carbon Nitride-Supported Single-Atom Iron Catalysts. *Nat Commun* **2024**, *15*, 8769. https://doi.org/10.1038/s41467-024-53055-1.
22. Martín, A.J.; Mondelli, C.; Jaydev, S.D.; Pérez-Ramírez, J. Catalytic Processing of Plastic Waste on the Rise. *Chem* **2021**, *7*, 1487–1533. https://doi.org/10.1016/j.chempr.2020.12.006.
23. Li, H.; Aguirre-Villegas, H.A.; Allen, R.D.; Bai, X.; Benson, C.H.; Beckham, G.T.; Bradshaw, S.L.; Brown, J.L.; Brown, R.C.; Cecon, V.S.; et al. Expanding Plastics Recycling Technologies: Chemical Aspects, Technology Status and Challenges. *Green Chemistry* **2022**, *24*, 8899–9002. https://doi.org/10.1039/D2GC02588D.
24. Jehanno, C.; Alty, J.W.; Roosen, M.; De Meester, S.; Dove, A.P.; Chen, E.Y.-X.; Leibfarth, F.A.; Sardon, H. Critical Advances and Future Opportunities in Upcycling Commodity Polymers. *Nature* **2022**, *603*, 803–814. https://doi.org/10.1038/s41586-021-04350-0.
25. Zhao, X.; Korey, M.; Li, K.; Copenhaver, K.; Tekinalp, H.; Celik, S.; Kalaitzidou, K.; Ruan, R.; Ragauskas, A.J.; Ozcan, S. Plastic Waste Upcycling toward a Circular Economy. *Chemical Engineering Journal* **2022**, *428*, 131928. https://doi.org/10.1016/j.cej.2021.131928.
26. Napper, I.E.; Davies, B.F.R.; Clifford, H.; Elvin, S.; Koldewey, H.J.; Mayewski, P.A.; Miner, K.R.; Potocki, M.; Elmore, A.C.; Gajurel, A.P.; et al. Reaching New Heights in Plastic Pollution—Preliminary Findings of Microplastics on Mount Everest. *One Earth* **2020**, *3*, 621–630. https://doi.org/10.1016/j.oneear.2020.10.020.
27. Bermúdez, J.R.; Swarzenski, P.W. A Microplastic Size Classification Scheme Aligned with Universal Plankton Survey Methods. *MethodsX* **2021**, *8*, 101516. https://doi.org/10.1016/j.mex.2021.101516.
28. Zimmermann, L.; Göttlich, S.; Oehlmann, J.; Wagner, M.; Völker, C. What Are the Drivers of Microplastic Toxicity? Comparing the Toxicity of Plastic Chemicals and Particles to Daphnia Magna. *Environmental Pollution* **2020**, *267*, 115392. https://doi.org/10.1016/j.envpol.2020.115392.
29. Guo, X.; Wang, J. The Chemical Behaviors of Microplastics in Marine Environment: A Review. *Mar Pollut Bull* **2019**, *142*, 1–14. https://doi.org/10.1016/j.marpolbul.2019.03.019.
30. Rafa, N.; Ahmed, B.; Zohora, F.; Bakya, J.; Ahmed, S.; Ahmed, S.F.; Mofijur, M.; Chowdhury, A.A.; Almomani, F. Microplastics as Carriers of Toxic Pollutants: Source, Transport, and Toxicological Effects. *Environmental Pollution* **2024**, *343*, 123190. https://doi.org/10.1016/j.envpol.2023.123190.
31. Hidalgo-Ruz, V.; Gutow, L.; Thompson, R.C.; Thiel, M. Microplastics in the Marine Environment: A Review of the Methods Used for Identification and Quantification. *Environ Sci Technol* **2012**, *46*, 3060–3075. https://doi.org/10.1021/es2031505.
32. Huang, Z.; Hu, B.; Wang, H. Analytical Methods for Microplastics in the Environment: A Review. *Environ Chem Lett* **2023**, *21*, 383–401. https://doi.org/10.1007/s10311-022-01525-7.

 doi:10.20944/preprints202509.1076.v1

33. Wang, Z.-M.; Wagner, J.; Ghosal, S.; Bedi, G.; Wall, S. SEM/EDS and Optical Microscopy Analyses of Microplastics in Ocean Trawl and Fish Guts. *Science of The Total Environment* **2017**, *603–604*, 616–626. https://doi.org/10.1016/j.scitotenv.2017.06.047.
34. Ivleva, N.P.; Wiesheu, A.C.; Niessner, R. Microplastic in Aquatic Ecosystems. *Angewandte Chemie International Edition* **2017**, *56*, 1720–1739. https://doi.org/10.1002/anie.201606957.
35. Primpke, S.; Lorenz, C.; Rascher-Friesenhausen, R.; Gerdts, G. An Automated Approach for Microplastics Analysis Using Focal Plane Array (FPA) FTIR Microscopy and Image Analysis. *Analytical Methods* **2017**, *9*, 1499–1511. https://doi.org/10.1039/C6AY02476A.
36. Araujo, C.F.; Nolasco, M.M.; Ribeiro, A.M.P.; Ribeiro-Claro, P.J.A. Identification of Microplastics Using Raman Spectroscopy: Latest Developments and Future Prospects. *Water Res* **2018**, *142*, 426–440. https://doi.org/10.1016/j.watres.2018.05.060.
37. Batel, A.; Borchert, F.; Reinwald, H.; Erdinger, L.; Braunbeck, T. Microplastic Accumulation Patterns and Transfer of Benzo[a]Pyrene to Adult Zebrafish (Danio Rerio) Gills and Zebrafish Embryos. *Environmental Pollution* **2018**, *235*, 918–930. https://doi.org/10.1016/j.envpol.2018.01.028.
38. Matsuguma, Y.; Takada, H.; Kumata, H.; Kanke, H.; Sakurai, S.; Suzuki, T.; Itoh, M.; Okazaki, Y.; Boonyatumanond, R.; Zakaria, M.P.; et al. Microplastics in Sediment Cores from Asia and Africa as Indicators of Temporal Trends in Plastic Pollution. *Arch Environ Contam Toxicol* **2017**, *73*, 230–239. https://doi.org/10.1007/s00244-017-0414-9.
39. Peez, N.; Janiska, M.-C.; Imhof, W. The First Application of Quantitative 1H NMR Spectroscopy as a Simple and Fast Method of Identification and Quantification of Microplastic Particles (PE, PET, and PS). *Anal Bioanal Chem* **2019**, *411*, 823–833. https://doi.org/10.1007/s00216-018-1510-z.
40. Zeng, G.; Zhao, B.; Deng, C.; Zhu, C.; Cheng, M.M.-C.; Gao, P.-X. Microplastic Detection and Monitoring in Biological and Environmental Systems: A Mini Review of Techniques and Strategies. *International Journal of High Speed Electronics and Systems* **2026**, *35*. https://doi.org/10.1142/S012915642640001X.
41. Cristoni, S.; Dusi, G.; Brambilla, P.; Albini, A.; Conti, M.; Brambilla, M.; Bruno, A.; Di Gaudio, F.; Ferlin, L.; Tazzari, V.; et al. SANIST: Optimization of a Technology for Compound Identification Based on the European Union Directive with Applications in Forensic, Pharmaceutical and Food Analyses. *Journal of Mass Spectrometry* **2017**, *52*, 16–21. https://doi.org/10.1002/jms.3895.
42. Elumalai, P. V.; Dhinesh, B.; Jayakar, J.; Nambiraj, M.; Hariharan, V. Effects of Antioxidants to Reduce the Harmful Pollutants from Diesel Engine Using Preheated Palm Oil–Diesel Blend. *J Therm Anal Calorim* **2022**, *147*, 2439–2453. https://doi.org/10.1007/s10973-021-10652-2.
43. Maddison, C.; Sathish, C.I.; Lakshmi, D.; Wayne, O.; Palanisami, T. An Advanced Analytical Approach to Assess the Long-Term Degradation of Microplastics in the Marine Environment. *Npj Mater Degrad* **2023**, *7*, 59. https://doi.org/10.1038/s41529-023-00377-y.
44. Pfohl, P.; Wagner, M.; Meyer, L.; Domercq, P.; Praetorius, A.; Hüffer, T.; Hofmann, T.; Wohlleben, W. Environmental Degradation of Microplastics: How to Measure Fragmentation Rates to Secondary Micro- and Nanoplastic Fragments and Dissociation into Dissolved Organics. *Environ Sci Technol* **2022**, *56*, 11323–11334. https://doi.org/10.1021/acs.est.2c01228.
45. Nene, A.; Sadeghzade, S.; Viaroli, S.; Yang, W.; Uchenna, U.P.; Kandwal, A.; Liu, X.; Somani, P.; Galluzzi, M. Recent Advances and Future Technologies in Nano-Microplastics Detection. *Environ Sci Eur* **2025**, *37*, 7. https://doi.org/10.1186/s12302-024-01044-y.
46. He, J.; Han, L.; Wang, F.; Ma, C.; Cai, Y.; Ma, W.; Xu, E.G.; Xing, B.; Yang, Z. Photocatalytic Strategy to Mitigate Microplastic Pollution in Aquatic Environments: Promising Catalysts, Efficiencies, Mechanisms, and Ecological Risks. *Crit Rev Environ Sci Technol* **2023**, *53*, 504–526. https://doi.org/10.1080/10643389.2022.2072658.
47. Wang, C.; Sun, R.; Huang, R.; Wang, H. Superior Fenton-like Degradation of Tetracycline by Iron Loaded Graphitic Carbon Derived from Microplastics: Synthesis, Catalytic Performance, and Mechanism. *Sep Purif Technol* **2021**, *270*, 118773. https://doi.org/10.1016/j.seppur.2021.118773.

 doi:10.20944/preprints202509.1076.v1

48. Ren, S.; Xu, X.; Zhu, Z.-S.; Yang, Y.; Tian, W.; Hu, K.; Zhong, S.; Yi, J.; Duan, X.; Wang, S. Catalytic Transformation of Microplastics to Functional Carbon for Catalytic Peroxymonosulfate Activation: Conversion Mechanism and Defect of Scavenging. *Appl Catal B* **2024**, *342*, 123410. https://doi.org/10.1016/j.apcatb.2023.123410.
49. Hou, Q.; Zhen, M.; Qian, H.; Nie, Y.; Bai, X.; Xia, T.; Laiq Ur Rehman, M.; Li, Q.; Ju, M. Upcycling and Catalytic Degradation of Plastic Wastes. *Cell Rep Phys Sci* **2021**, *2*, 100514. https://doi.org/10.1016/j.xcrp.2021.100514.
50. Jeyaraj, J.; Baskaralingam, V.; Stalin, T.; Muthuvel, I. Mechanistic Vision on Polypropylene Microplastics Degradation by Solar Radiation Using TiO2 Nanoparticle as Photocatalyst. *Environ Res* **2023**, *233*, 116366. https://doi.org/10.1016/j.envres.2023.116366.
51. Wan, Y.; Wang, H.; Huo, P. Plastic Degradation and Conversion by Photocatalysis. In; 2024; pp. 1–22.
52. Wang, X.; Zhu, Z.; Jiang, J.; Li, R.; Xiong, J. Preparation of Heterojunction C3N4/WO3 Photocatalyst for Degradation of Microplastics in Water. *Chemosphere* **2023**, *337*, 139206. https://doi.org/10.1016/j.chemosphere.2023.139206.
53. Liu, X.; Yang, Z.; Liu, H.; Li, Y.; Zhang, G. Efficient Photocatalytic Degradation of Microplastics by Constructing a Novel Z-Scheme Fe-Doped BiO2−x/BiOI Heterojunction with Full-Spectrum Response: Mechanistic Insights and Theory Calculations. *J Hazard Mater* **2024**, *480*, 136080. https://doi.org/10.1016/j.jhazmat.2024.136080.
54. Xie, A.; Jin, M.; Zhu, J.; Zhou, Q.; Fu, L.; Wu, W. Photocatalytic Technologies for Transformation and Degradation of Microplastics in the Environment: Current Achievements and Future Prospects. *Catalysts* **2023**, *13*, 846. https://doi.org/10.3390/catal13050846.
55. Zhu, C.; Wang, X. Nanomaterial ZnO Synthesis and Its Photocatalytic Applications: A Review. *Nanomaterials* **2025**, *15*, 682. https://doi.org/10.3390/nano15090682.
56. Surana, M.; Pattanayak, D.S.; Yadav, V.; Singh, V.K.; Pal, D. An Insight Decipher on Photocatalytic Degradation of Microplastics: Mechanism, Limitations, and Future Outlook. *Environ Res* **2024**, *247*, 118268. https://doi.org/10.1016/j.envres.2024.118268.
57. Kang, S.; Sun, T.; Ma, Y.; Du, M.; Gong, M.; Zhou, C.; Chai, Y.; Qiu, B. Artificial Photosynthesis Bringing New Vigor into Plastic Wastes. *SmartMat* **2023**, *4*. https://doi.org/10.1002/smm2.1202.
58. Zhang, C.; Huang, L.; Nekliudov, A. Construction of Loading G-C3N4/TiO2 on Waste Cotton-Based Activated Carbon S-Scheme Heterojunction for Enhanced Photocatalytic Degradation of Microplastics: Performance, DFT Calculation and Mechanism Study. *Opt Mater (Amst)* **2024**, *154*, 115786. https://doi.org/10.1016/j.optmat.2024.115786.
59. Wang, X.; Zhu, Z.; Jiang, J.; Li, R.; Xiong, J. Preparation of Heterojunction C3N4/WO3 Photocatalyst for Degradation of Microplastics in Water. *Chemosphere* **2023**, *337*, 139206. https://doi.org/10.1016/j.chemosphere.2023.139206.
60. Cao, B.; Wan, S.; Wang, Y.; Guo, H.; Ou, M.; Zhong, Q. Highly-Efficient Visible-Light-Driven Photocatalytic H2 Evolution Integrated with Microplastic Degradation over MXene/ZnxCd1-XS Photocatalyst. *J Colloid Interface Sci* **2022**, *605*, 311–319. https://doi.org/10.1016/j.jcis.2021.07.113.
61. Maulana, D.A.; Ibadurrohman, M.; Slamet Synthesis of Nano-Composite Ag/TiO ₂ for Polyethylene Microplastic Degradation Applications. *IOP Conf Ser Mater Sci Eng* **2021**, *1011*, 012054. https://doi.org/10.1088/1757-899X/1011/1/012054.
62. Tofa, T.S.; Ye, F.; Kunjali, K.L.; Dutta, J. Enhanced Visible Light Photodegradation of Microplastic Fragments with Plasmonic Platinum/Zinc Oxide Nanorod Photocatalysts. *Catalysts* **2019**, *9*, 819. https://doi.org/10.3390/catal9100819.
63. Yang, Z.; Wang, H.; Li, Y.; Zhang, G. Efficient Photocatalytic Degradation of Polystyrene Microplastics in Water over Core–Shell BiO2−x/CuBi2O4 Heterojunction with Full Spectrum Light Response. *J Colloid Interface Sci* **2025**, *686*, 327–335. https://doi.org/10.1016/j.jcis.2025.01.242.
64. Liu, J.; Zhao, D.; Wu, X.; Wu, D.; Su, N.; Wang, Y.; Chen, F.; Fu, C.; Wang, J.; Zhang, Q. Synergistic Dual-Defect Band Engineering for Highly Efficient Photocatalytic Degradation of Microplastics *via* Nb-Induced Oxygen Vacancies in SnO ₂ Quantum Dots. *J Mater Chem A Mater* **2025**, *13*, 4429–4443. https://doi.org/10.1039/D4TA07579J.

 doi:10.20944/preprints202509.1076.v1

65. Quilumbaquin, W.; Castillo-Cabrera, G.X.; Borrero-González, L.J.; Mora, J.R.; Valle, V.; Debut, A.; Loor-Urgilés, L.D.; Espinoza-Montero, P.J. Photoelectrocatalytic Degradation of High-Density Polyethylene Microplastics on TiO2-Modified Boron-Doped Diamond Photoanode. *iScience* **2024**, *27*, 109192. https://doi.org/10.1016/j.isci.2024.109192.
66. Lin, L.; Yi, J.; Wang, J.; Qian, Q.; Chen, Q.; Cao, C.; Zhou, W. Enhancing Microplastic Degradation through Synergistic Photocatalytic and Pretreatment Approaches. *Langmuir* **2024**, *40*, 22582–22590. https://doi.org/10.1021/acs.langmuir.4c02124.
67. He, Y.; Rehman, A.U.; Xu, M.; Not, C.A.; Ng, A.M.C.; Djurišić, A.B. Photocatalytic Degradation of Different Types of Microplastics by TiOx/ZnO Tetrapod Photocatalysts. *Heliyon* **2023**, *9*, e22562. https://doi.org/10.1016/j.heliyon.2023.e22562.
68. Jiang, R.; Lu, G.; Dang, T.; Wang, M.; Liu, J.; Yan, Z.; Xie, H. Insight into the Degradation Process of Functional Groups Modified Polystyrene Microplastics with Dissolvable BiOBr-OH Semiconductor-Organic Framework. *Chemical Engineering Journal* **2023**, *470*, 144401. https://doi.org/10.1016/j.cej.2023.144401.
69. Nguyen, T.T.; Hidalgo-Jiménez, J.; Sauvage, X.; Saito, K.; Guo, Q.; Edalati, K. Phase and Sulfur Vacancy Engineering in Cadmium Sulfide for Boosting Hydrogen Production from Catalytic Plastic Waste Photoconversion. *Chemical Engineering Journal* **2025**, *504*, 158730. https://doi.org/10.1016/j.cej.2024.158730.
70. Xiao, Y.; Tian, Y.; Xu, W.; Zhu, J. Photodegradation of Microplastics through Nanomaterials: Insights into Photocatalysts Modification and Detailed Mechanisms. *Materials* **2024**, *17*, 2755. https://doi.org/10.3390/ma17112755.
71. Wan, Y.; Wang, H.; Huo, P. Plastic Degradation and Conversion by Photocatalysis. In; 2024; pp. 1–22.
72. Zhou, G.; Xu, H.; Song, H.; Yi, J.; Wang, X.; Chen, Z.; Zhu, X. Photocatalysis toward Microplastics Conversion: A Critical Review. *ACS Catal* **2024**, *14*, 8694–8719. https://doi.org/10.1021/acscatal.4c01449.
73. Gu, X.; Li, L.; Wu, Y.; Dong, W. Enhancement of Microplastics Degradation with MIL-101 Modified BiOI Photocatalyst under Light and Dark Alternated System. *J Environ Chem Eng* **2024**, *12*, 112958. https://doi.org/10.1016/j.jece.2024.112958.
74. Meng, Z.; Sun, C.; Wang, C.; Wang, Z.; Deng, S.; Yang, H. Boosting Photocatalytic Capability by Dispersing TiO2 into Chitin Matrix for Polystyrene Microplastics Degradation. *Appl Surf Sci* **2025**, *711*, 164104. https://doi.org/10.1016/j.apsusc.2025.164104.
75. Liu, Y.; Wang, J. Multivalent Metal Catalysts in Fenton/Fenton-like Oxidation System: A Critical Review. *Chemical Engineering Journal* **2023**, *466*, 143147. https://doi.org/10.1016/j.cej.2023.143147.
76. Liu, Y.; Zhao, Y.; Wang, J. Fenton/Fenton-like Processes with in-Situ Production of Hydrogen Peroxide/Hydroxyl Radical for Degradation of Emerging Contaminants: Advances and Prospects. *J Hazard Mater* **2021**, *404*, 124191. https://doi.org/10.1016/j.jhazmat.2020.124191.
77. Meyerstein, D. Re-Examining Fenton and Fenton-like Reactions. *Nat Rev Chem* **2021**, *5*, 595–597. https://doi.org/10.1038/s41570-021-00310-4.
78. Xiao, J.; Guo, S.; Wang, D.; An, Q. Fenton-Like Reaction: Recent Advances and New Trends. *Chemistry – A European Journal* **2024**, *30*. https://doi.org/10.1002/chem.202304337.
79. Zarghami Qaretapeh, M.; Kouchakipour, S.; Hosseinzadeh, M.; Dashtian, K. Cuttlefish Bone-Supported CoFe2O4 Nanoparticles Enhance Persulfate Fenton-like Process for the Degradation of Polystyrene Nanoplastics. *Chemical Engineering Journal* **2024**, *490*, 151833. https://doi.org/10.1016/j.cej.2024.151833.
80. Ye, J.; Li, N.; Gao, W.; Peng, W.; Peng, X.; Cheng, Z.; Yan, B.; Fu, Y.; Zhan, S.; Chen, G.; et al. Bimetal-Carbon Engineering for Polypropylene Conversion into Hydrocarbons and Ketones in a Fenton-like System. *Applied Catalysis B: Environment and Energy* **2024**, *358*, 124411. https://doi.org/10.1016/j.apcatb.2024.124411.
81. Camilli, E.; Pighin, A.F.; Copello, G.J.; Villanueva, M.E. Cobalt/Carbon Quantum Dots Core-Shell Nanoparticles as an Improved Catalyst for Fenton-like Reaction. *Nano-Structures & Nano-Objects* **2024**, *37*, 101097. https://doi.org/10.1016/j.nanoso.2024.101097.
82. Ye, Q.; Xu, H.; Hunter, T.N.; Harbottle, D.; Kale, G.M.; Tillotson, M.R. Advanced Polystyrene Nanoplastic Remediation through Electro-Fenton Process: Degradation Mechanisms and Pathways. *J Environ Chem Eng* **2025**, *13*, 118907. https://doi.org/10.1016/j.jece.2025.118907.

83. Wu, M.; Wang, R.; Miao, L.; Sun, P.; Zhou, B.; Xiong, Y.; Dong, X. Synergistically Piezocatalytic and Fenton-like Activation of H2O2 by a Ferroelectric Bi12(Bi0.5Fe0.5)O19.5 Catalyst to Boost Degradation of Polyethylene Terephthalate Microplastic (PET-MPs). *J Colloid Interface Sci* **2025**, *682*, 738–750. https://doi.org/10.1016/j.jcis.2024.12.002.
84. Xue, Z.; Yu, X.; Ke, X.; Zhao, J. A Novel Route for Microplastic Mineralization: Visible-Light-Driven Heterogeneous Photocatalysis and Photothermal Fenton-like Reaction. *Environ Sci Nano* **2024**, *11*, 113–122. https://doi.org/10.1039/D3EN00642E.
85. Hu, K.; Zhou, P.; Yang, Y.; Hall, T.; Nie, G.; Yao, Y.; Duan, X.; Wang, S. Degradation of Microplastics by a Thermal Fenton Reaction. *ACS ES&T Engineering* **2022**, *2*, 110–120. https://doi.org/10.1021/acsestengg.1c00323.
86. Zanaty, M.; Zaki, A.H.; El-Dek, S.I.; Abdelhamid, H.N. Zeolitic Imidazolate Framework@hydrogen Titanate Nanotubes for Efficient Adsorption and Catalytic Oxidation of Organic Dyes and Microplastics. *J Environ Chem Eng* **2024**, *12*, 112547. https://doi.org/10.1016/j.jece.2024.112547.
87. Bule Možar, K.; Milološa, M.; Martinjak, V.; Radovanović-Perić, F.; Bafti, A.; Ujević Bošnjak, M.; Markić, M.; Bolanča, T.; Cvetnić, M.; Kučić Grgić, D.; et al. Evaluation of Fenton, Photo-Fenton and Fenton-like Processes in Degradation of PE, PP, and PVC Microplastics. *Water (Basel)* **2024**, *16*, 673. https://doi.org/10.3390/w16050673.
88. Shen, M.; Song, B.; Zhou, C.; Hu, T.; Zeng, G.; Zhang, Y. Advanced Oxidation Processes for the Elimination of Microplastics from Aqueous Systems: Assessment of Efficiency, Perspectives and Limitations. *Science of The Total Environment* **2022**, *842*, 156723. https://doi.org/10.1016/j.scitotenv.2022.156723.
89. Wang, J.; Sun, C.; Huang, Q.-X.; Chi, Y.; Yan, J.-H. Adsorption and Thermal Degradation of Microplastics from Aqueous Solutions by Mg/Zn Modified Magnetic Biochars. *J Hazard Mater* **2021**, *419*, 126486. https://doi.org/10.1016/j.jhazmat.2021.126486.
90. Nabgan, W.; Nabgan, B.; Tuan Abdullah, T.A.; Ikram, M.; Jadhav, A.H.; Jalil, A.A.; Ali, M.W. Highly Active Biphasic Anatase-Rutile Ni-Pd/TNPs Nanocatalyst for the Reforming and Cracking Reactions of Microplastic Waste Dissolved in Phenol. *ACS Omega* **2022**, *7*, 3324–3340. https://doi.org/10.1021/acsomega.1c05488.
91. Ma, S.; Tang, S.; Zhao, Y. Upcycling Polystyrene Microplastics to Fe/Mo-Doped Sponge-Carbon: Mo5+ Enhanced Electron Transfer for Boosting Fenton-like Performance. *Chemical Engineering Journal* **2024**, *498*, 155460. https://doi.org/10.1016/j.cej.2024.155460.
92. Sun, R.; Yang, J.; Huang, R.; Wang, C. Controlled Carbonization of Microplastics Loaded Nano Zero-Valent Iron for Catalytic Degradation of Tetracycline. *Chemosphere* **2022**, *303*, 135123. https://doi.org/10.1016/j.chemosphere.2022.135123.
93. Ren, S.; Xu, X.; Zhu, Z.-S.; Yang, Y.; Tian, W.; Hu, K.; Zhong, S.; Yi, J.; Duan, X.; Wang, S. Catalytic Transformation of Microplastics to Functional Carbon for Catalytic Peroxymonosulfate Activation: Conversion Mechanism and Defect of Scavenging. *Appl Catal B* **2024**, *342*, 123410. https://doi.org/10.1016/j.apcatb.2023.123410.
94. Hao, Y.; Che, X.; Hou, X.; Shi, L.; Huang, L. Recent Advances in the Thermo-Catalytic Upcycling of Polyethylene Waste. *ACS Appl Polym Mater* **2025**, *7*, 6597–6612. https://doi.org/10.1021/acsapm.5c01083.
95. Wang, H.; Chen, H.; Wan, Q.; Zheng, Y.; Wan, Y.; Liu, X.; Song, X.; Ma, W.; Huo, P. Catalytic Degradation of Polyethylene Terephthalate Microplastics by Co-N/C@CeO2 Composite in Thermal-Assisted Activation PMS System: Process Mechanism and Toxicological Analysis. *Chemical Engineering Journal* **2025**, *514*, 163192. https://doi.org/10.1016/j.cej.2025.163192.
96. Vo, T.-P.; Rintala, J.; Dai, L.; Oh, W.-D.; He, C. The Role of Ubiquitous Metal Ions in Degradation of Microplastics in Hot-Compressed Water. *Water Res* **2023**, *245*, 120672. https://doi.org/10.1016/j.watres.2023.120672.
97. Daligaux, V.; Richard, R.; Manero, M.-H. Deactivation and Regeneration of Zeolite Catalysts Used in Pyrolysis of Plastic Wastes—A Process and Analytical Review. *Catalysts* **2021**, *11*, 770. https://doi.org/10.3390/catal11070770.

 doi:10.20944/preprints202509.1076.v1

98. RAZALI, N.; WAN ABDULLAH, W.R.; MOHD ZIKIR, N. EFFECT OF THERMO-PHOTOCATALYTIC PROCESS USING ZINC OXIDE ON DEGRADATION OF MACRO/MICRO-PLASTIC IN AQUEOUS ENVIRONMENT. *J Sustain Sci Manag* **2020**, *15*, 1–14. https://doi.org/10.46754/jssm.2020.08.001.
99. Jiao, Y.; Wang, S.; Sun, B.; Han, Y.; Zhang, Z.; Shen, X.; Li, Z. Adsorption Efficiency and In-Situ Catalytic Thermal Degradation Behaviour of Microplastics from Water over Fe-Modified Lignin-Based Magnetic Biochar. *Sep Purif Technol* **2025**, *353*, 128468. https://doi.org/10.1016/j.seppur.2024.128468.
100. Li, S.; Yang, Y.; Yang, S.; Zheng, H.; Zheng, Y.; M, J.; Nagarajan, D.; Varjani, S.; Chang, J.-S. Recent Advances in Biodegradation of Emerging Contaminants - Microplastics (MPs): Feasibility, Mechanism, and Future Prospects. *Chemosphere* **2023**, *331*, 138776. https://doi.org/10.1016/j.chemosphere.2023.138776.
101. Gao, W.; Xu, M.; Zhao, W.; Yang, X.; Xin, F.; Dong, W.; Jia, H.; Wu, X. Microbial Degradation of (Micro)Plastics: Mechanisms, Enhancements, and Future Directions. *Fermentation* **2024**, *10*, 441. https://doi.org/10.3390/fermentation10090441.
102. Thakur, B.; Singh, J.; Singh, J.; Angmo, D.; Vig, A.P. Biodegradation of Different Types of Microplastics: Molecular Mechanism and Degradation Efficiency. *Science of The Total Environment* **2023**, *877*, 162912. https://doi.org/10.1016/j.scitotenv.2023.162912.
103. Du, H.; Xie, Y.; Wang, J. Microplastic Degradation Methods and Corresponding Degradation Mechanism: Research Status and Future Perspectives. *J Hazard Mater* **2021**, *418*, 126377. https://doi.org/10.1016/j.jhazmat.2021.126377.
104. Rincon, I.; Hidalgo, T.; Armani, G.; Rojas, S.; Horcajada, P. Enzyme_Metal-Organic Framework Composites as Novel Approach for Microplastic Degradation. *ChemSusChem* **2024**. https://doi.org/10.1002/cssc.202301350.
105. Zandieh, M.; Liu, J. Removal and Degradation of Microplastics Using the Magnetic and Nanozyme Activities of Bare Iron Oxide Nanoaggregates. *Angewandte Chemie* **2022**, *134*. https://doi.org/10.1002/ange.202212013.
106. Yang, Y.; Chen, J.; Chen, Z.; Yu, Z.; Xue, J.; Luan, T.; Chen, S.; Zhou, S. Mechanisms of Polystyrene Microplastic Degradation by the Microbially Driven Fenton Reaction. *Water Res* **2022**, *223*, 118979. https://doi.org/10.1016/j.watres.2022.118979.
107. Zhang, A.; Hou, Y.; Hou, S.; Wang, Y.; Wang, Q. Enhancement of Microplastics Degradation Efficiency: Microbial Laccase-Driven Radical Chemical Coupling Catalysis. *Chemical Engineering Journal* **2025**, *507*, 160579. https://doi.org/10.1016/j.cej.2025.160579.
108. Li, X.; Li, G.; Wang, J.; Li, X.; Yang, Y.; Song, D. Elucidating Polyethylene Microplastic Degradation Mechanisms and Metabolic Pathways via Iron-Enhanced Microbiota Dynamics in Marine Sediments. *J Hazard Mater* **2024**, *466*, 133655. https://doi.org/10.1016/j.jhazmat.2024.133655.
109. Wan, P.; Chen, G.; Fan, J.; Tan, W.; Li, X.; Chen, L.; Li, K. Modulating Ion Migration Realizes Both Enhanced and Long-Term-Stable Nanozyme Activity for Efficient Microplastic Degradation. *Chem Sci* **2025**. https://doi.org/10.1039/D5SC04247J.
110. Ren, J.; Meng, Y.; Wang, Z.; Xie, G. Degradation of Microplastics by Microbial in Combination with a Micromotor. *ACS Sustain Chem Eng* **2025**, *13*, 4018–4027. https://doi.org/10.1021/acssuschemeng.4c09593.
111. Huang, Q.-S.; Chen, S.-Q.; Zhao, X.-M.; Song, L.-J.; Deng, Y.-M.; Xu, K.-W.; Yan, Z.-F.; Wu, J. Enhanced Degradation of Polyethylene Terephthalate (PET) Microplastics by an Engineered Stenotrophomonas Pavanii in the Presence of Biofilm. *Science of The Total Environment* **2024**, *955*, 177129. https://doi.org/10.1016/j.scitotenv.2024.177129.
112. Wan, P.; Chen, G.; Fan, J.; Tan, W.; Li, X.; Chen, L.; Li, K. Modulating Ion Migration Realizes Both Enhanced and Long-Term-Stable Nanozyme Activity for Efficient Microplastic Degradation. *Chem Sci* **2025**. https://doi.org/10.1039/D5SC04247J.
113. Shao, D.; Zhao, W.; Ji, S.; Yang, C.; Zhang, J.; Guo, R.; Zhang, B.; Lyu, W.; Feng, J.; Xu, H.; et al. Joule Heat Assisting Electrochemical Degradation of Polyethylene Microplastics Melted on Anode. *Applied Catalysis B: Environment and Energy* **2024**, *357*, 124281. https://doi.org/10.1016/j.apcatb.2024.124281.
114. Mao, Y.; Fan, S.; Li, X.; Shi, J.; Wang, M.; Niu, Z.; Chen, G. Trash to Treasure: Electrocatalytic Upcycling of Polyethylene Terephthalate (PET) Microplastic to Value-Added Products by Mn0.1Ni0.9Co2O4-δ RSFs Spinel. *J Hazard Mater* **2023**, *457*, 131743. https://doi.org/10.1016/j.jhazmat.2023.131743.

115. Zheng, W.; Liu, Z.; Wang, B.; Tao, M.; Ji, H.; Xiang, X.; Fu, Z.; Liao, L.; Liao, P.; Chen, R. Effective Degradation of Polystyrene Microplastics by Ti/La/Co-Sb-SnO2 Anodes: Enhanced Electrocatalytic Stability and Electrode Lifespan. *Science of The Total Environment* **2024**, *922*, 171002. https://doi.org/10.1016/j.scitotenv.2024.171002.
116. Zheng, W.; Wang, B.; Liu, Z.; Yang, H.; Chen, Z.; Sun, X. La-Doped Ti/Sb-SnO2 Electrode Enhanced Removal of Microplastics by Advanced Electrocatalysis Oxidation Process (AEOP) Strategy. *Desalination Water Treat* **2024**, *320*, 100622. https://doi.org/10.1016/j.dwt.2024.100622.
117. Ning, Z.; Duan, X.; Li, Y.; Zhao, X.; Chang, L. Degradation of Polyvinyl Chloride Microplastics via Electrochemical Oxidation with a CeO2–PbO2 Anode. *J Clean Prod* **2023**, *432*, 139668. https://doi.org/10.1016/j.jclepro.2023.139668.
118. Ma, F.; Wang, S.; Gong, X.; Liu, X.; Wang, Z.; Wang, P.; Liu, Y.; Cheng, H.; Dai, Y.; Zheng, Z.; et al. Highly Efficient Electrocatalytic Hydrogen Evolution Coupled with Upcycling of Microplastics in Seawater Enabled via Ni3N/W5N4 Janus Nanostructures. *Appl Catal B* **2022**, *307*, 121198. https://doi.org/10.1016/j.apcatb.2022.121198.
119. Kuila, S.K.; Dhanda, A.; Samal, B.; Ghangrekar, M.M.; Dubey, B.K.; Kundu, T.K. Defect Engineered 2D Graphitic Carbon Nitride for Photochemical, (Bio)Electrochemical, and Microplastic Remediation Advancements. *ACS ES&T Water* **2024**, *4*, 4283–4298. https://doi.org/10.1021/acsestwater.4c00478.
120. Wang, Y.; Zhong, H.; Xu, Q.; Dong, M.; Yang, J.; Yang, W.; Feng, Y.; Su, Z.-M. Vacancy-Rich NiFe-LDH/Carbon Paper as a Novel Self-Supporting Electrode for the Electro-Fenton Degradation of Polyvinyl Chloride Microplastics. *J Hazard Mater* **2025**, *485*, 136797. https://doi.org/10.1016/j.jhazmat.2024.136797.
121. Miranda Zoppas, F.; Sacco, N.; Soffietti, J.; Devard, A.; Akhter, F.; Marchesini, F.A. Catalytic Approaches for the Removal of Microplastics from Water: Recent Advances and Future Opportunities. *Chemical Engineering Journal Advances* **2023**, *16*, 100529. https://doi.org/10.1016/j.ceja.2023.100529.
122. Ye, J.; Chen, Y.; Gao, C.; Wang, C.; Hu, A.; Dong, G.; Chen, Z.; Zhou, S.; Xiong, Y. Sustainable Conversion of Microplastics to Methane with Ultrahigh Selectivity by a Biotic–Abiotic Hybrid Photocatalytic System. *Angewandte Chemie* **2022**, *134*. https://doi.org/10.1002/ange.202213244.
123. Kang, J.; Zhou, L.; Duan, X.; Sun, H.; Ao, Z.; Wang, S. Degradation of Cosmetic Microplastics via Functionalized Carbon Nanosprings. *Matter* **2019**, *1*, 745–758. https://doi.org/10.1016/j.matt.2019.06.004.
124. Miao, F.; Liu, Y.; Gao, M.; Yu, X.; Xiao, P.; Wang, M.; Wang, S.; Wang, X. Degradation of Polyvinyl Chloride Microplastics via an Electro-Fenton-like System with a TiO2/Graphite Cathode. *J Hazard Mater* **2020**, *399*, 123023. https://doi.org/10.1016/j.jhazmat.2020.123023.
125. Lu, Y.; Dong, Y.; Liu, W.; Jin, Q.; Lin, H. Piezo-Photocatalytic Enhanced Microplastic Degradation on Hetero-Interpenetrated Fe1−xS/FeMoO4/ MoS2 by Producing H2O2 and Self-Fenton Action. *Chemical Engineering Journal* **2025**, *508*, 160935. https://doi.org/10.1016/j.cej.2025.160935.
126. Kim, J.; Jang, J.; Hilberath, T.; Hollmann, F.; Park, C.B. Photoelectrocatalytic Biosynthesis Fuelled by Microplastics. *Nature Synthesis* **2022**, *1*, 776–786. https://doi.org/10.1038/s44160-022-00153-x.
127. Feng, Z.-Y.; Jiang, J.-C.; Jin, B.; Meng, L.-Y. Hydrogen Evolution Coupled with Microplastic Upcycling in Seawater via Solvent-Free Plasma F-Functionalized CoNi Alloy Catalysts. *J Alloys Compd* **2024**, *1008*, 176593. https://doi.org/10.1016/j.jallcom.2024.176593.
128. Shao, D.; Zhao, W.; Ji, S.; Yang, C.; Zhang, J.; Guo, R.; Zhang, B.; Lyu, W.; Feng, J.; Xu, H.; et al. Joule Heat Assisting Electrochemical Degradation of Polyethylene Microplastics Melted on Anode. *Applied Catalysis B: Environment and Energy* **2024**, *357*, 124281. https://doi.org/10.1016/j.apcatb.2024.124281.
129. Efremenko, E.N.; Lyagin, I. V.; Maslova, O. V.; Senko, O. V.; Stepanov, N.A.; Aslanli, A.G.G. Catalytic Degradation of Microplastics. *Russian Chemical Reviews* **2023**, *92*, RCR5069. https://doi.org/10.57634/RCR5069.
130. Zandieh, M.; Griffiths, E.; Waldie, A.; Li, S.; Honek, J.; Rezanezhad, F.; Van Cappellen, P.; Liu, J. Catalytic and Biocatalytic Degradation of Microplastics. *Exploration* **2024**, *4*. https://doi.org/10.1002/EXP.20230018.
131. Du, H.; Xie, Y.; Wang, J. Microplastic Degradation Methods and Corresponding Degradation Mechanism: Research Status and Future Perspectives. *J Hazard Mater* **2021**, *418*, 126377. https://doi.org/10.1016/j.jhazmat.2021.126377.

 doi:10.20944/preprints202509.1076.v1

132. Gao, W.; Zhang, Y.; Mo, A.; Jiang, J.; Liang, Y.; Cao, X.; He, D. Removal of Microplastics in Water: Technology Progress and Green Strategies. *Green Analytical Chemistry* **2022**, *3*, 100042. https://doi.org/10.1016/j.greeac.2022.100042.
133. Hettiarachchi, H.; Meegoda, J.N. Microplastic Pollution Prevention: The Need for Robust Policy Interventions to Close the Loopholes in Current Waste Management Practices. *Int J Environ Res Public Health* **2023**, *20*, 6434. https://doi.org/10.3390/ijerph20146434.
134. Koelmans, A.A.; Redondo-Hasselerharm, P.E.; Nor, N.H.M.; de Ruijter, V.N.; Mintenig, S.M.; Kooi, M. Risk Assessment of Microplastic Particles. *Nat Rev Mater* **2022**, *7*, 138–152. https://doi.org/10.1038/s41578-021-00411-y.
135. Xayachak, T.; Haque, N.; Lau, D.; Pramanik, B.K. The Missing Link: A Systematic Review of Microplastics and Its Neglected Role in Life-Cycle Assessment. *Science of The Total Environment* **2024**, *954*, 176513. https://doi.org/10.1016/j.scitotenv.2024.176513.
136. Mohamed Nor, N.H.; Kooi, M.; Diepens, N.J.; Koelmans, A.A. Lifetime Accumulation of Microplastic in Children and Adults. *Environ Sci Technol* **2021**, *55*, 5084–5096. https://doi.org/10.1021/acs.est.0c07384.